**Title:** Biophysical potential and uncertainties of global seaweed farming

This manuscript has been submitted for publication in Nature Geoscience. Please note that this version of the manuscript has not been peer-reviewed. Subsequent versions of this manuscript may have slightly different content.

The supplementary material has been appended to the end of the main manuscript.

**Contact information for all authors:**

**1) Isabella B. Arzeno-Soltero**
**Institution**: Department of Civil & Environmental Engineering, University of California at Irvine, Irvine, CA
**Email**: iarzeno@uci.edu
*Corresponding author

**2) Christina Frieder**
**Institution**: Southern California Coastal Water Research Project, Costa Mesa, CA
**Email**: christinaf@sccwrp.org

**3) Benjamin Saenz**
**Institution**: biota.earth, Berkeley, CA
**Email**: blsaenz@gmail.com

**4) Matthew Long**
**Institution**: National Center for Atmospheric Research, Boulder, CO
**Email**: mclong@ucar.edu

**5) Julianne DeAngelo**
**Institution**: Department of Earth System Science, University of California at Irvine, Irvine, CA
**Email**: deangelj@uci.edu

**6) Steven J. Davis**
**Institution**: Department of Earth System Science, University of California at Irvine, Irvine, CA
**Email**: sjdavis@uci.edu

**7) Kristen Davis**
**Institution**: Department of Civil & Environmental Engineering, University of California at Irvine, Irvine, CA
**Email**: davis@uci.edu
*Corresponding author

**Title:** Biophysical potential and uncertainties of global seaweed farming

This manuscript has been submitted for publication in Nature Geoscience. Please note that this version of the manuscript has not been peer-reviewed. Subsequent versions of this manuscript may have slightly different content.

**Contact information for all authors:**

**1) Isabella B. Arzeno-Soltero**
**Institution**: Department of Civil & Environmental Engineering, University of California at Irvine, Irvine, CA
**Email**: iarzeno@uci.edu
*Corresponding author

**2) Christina Frieder**
**Institution**: Southern California Coastal Water Research Project, Costa Mesa, CA
**Email**: christinaf@sccwrp.org

**3) Benjamin Saenz**
**Institution**: biota.earth, Berkeley, CA
**Email**: blsaenz@gmail.com

**4) Matthew Long**
**Institution**: National Center for Atmospheric Research, Boulder, CO
**Email**: mclong@ucar.edu

**5) Julianne DeAngelo**
**Institution**: Department of Earth System Science, University of California at Irvine, Irvine, CA
**Email**: deangelj@uci.edu

**6) Steven J. Davis**
**Institution**: Department of Earth System Science, University of California at Irvine, Irvine, CA
**Email**: sjdavis@uci.edu

**7) Kristen Davis**
**Institution**: Department of Civil & Environmental Engineering, University of California at Irvine, Irvine, CA
**Email**: davis@uci.edu
*Corresponding author

# Biophysical potential and uncertainties of global seaweed farming

**Isabella B. Arzeno-Soltero[1,*], Christina Frieder[2], Benjamin T. Saenz[3], Matthew C. Long[4], Julianne DeAngelo[5], Steven J. Davis[5,1], and Kristen A. Davis[1,5,*]**

[1]Department of Civil and Environmental Engineering, UC Irvine, Irvine, CA
[2]Southern California Coastal Water Research Project, Costa Mesa, CA
[3]biota.earth, Berkeley, CA
[4]National Center for Atmospheric Research, Boulder, CO
[5]Department of Earth System Science, UC Irvine, Irvine, CA
[*]iarzeno@uci.edu, davis@uci.edu

## ABSTRACT

International climate goals require over 5 gigatons/year (Gt/year) of $CO_2$ to be removed from the atmosphere by midcentury. Macroalgae mariculture has been proposed as a strategy for such carbon dioxide removal (CDR). However, the global potential for seaweed cultivation has not been assessed in detail. Here, we develop and use a dynamic seaweed growth model, the Global MacroAlgae Cultivation MODeling System (G-MACMODS), to estimate potential yields of four different types of seaweed worldwide, and test the sensitivity of these estimates to uncertain biophysical parameters under two nutrient scenarios (one in which the surface ocean nutrient budget is unaltered by the presence of seaweed farms, and another in which seaweed harvest is limited by nutrients that are resupplied by vertical transport). We find that 1 Gt of seaweed carbon could be harvested in 0.8% of global exclusive economic zones (EEZs; equivalent to $\sim$1 million km$^2$) if farms were located in the most productive areas, but potential harvest estimates are highly uncertain due to ill-constrained seaweed mortality and nitrogen exudation rates. Our results suggest that seaweed farming could produce climate-relevant quantities of biomass carbon and highlight key uncertainties to be resolved by future research.

Recent analysis of global climate scenarios suggests that limiting warming to $< 1.5^\circ$ above pre-industrial levels will require large reductions in $CO_2$ emissions as well as the removal of 4-14 Gt-$CO_2$/year by midcentury[1,2]. The ocean operates as a natural sink for $CO_2$, having absorbed 26% of anthropogenic $CO_2$ emitted in the last century[3,4]. There is increasing interest in enhancing ocean carbon dioxide removal (CDR) through seaweed farming - where surface carbon, fixed in seaweed biomass, is sunk and sequestered in the deep ocean[5–7]. In contrast to terrestrial biomass, seaweed farming does not require arable land or freshwater. Moreover, farmed seaweed may be used for biofuel production[8–10], animal feed[11,12], and bioremediation[13–16], while also providing ecosystem services[17]. Annual production of seaweed increased by an average of 50% between 2010 and 2015, with 3.2 Mt of dry weight ($\sim$1 MtC) harvested globally in 2018[18]. Although most farming today occurs in coastal areas of China and Indonesia, technology to farm offshore is quickly evolving[19–23].

Previous assessments of the global potential of farmed seaweed to remove carbon, though noteworthy, have generally extrapolated from observed yields in high-nutrient regions[5–7,15,24] or average global productivity of wild seaweeds[25], disregarding spatial variations in hydrodynamics, nutrient fluxes, and parameter uncertainty. Meanwhile, dynamic models of seaweed growth under nutrient and other environmental limitations[26–30] have often focused on relatively small ($< 500$ km$^2$) coastal areas and have not examined the levels of intensive nutrient uptake required to produce biomass at scales relevant to the global carbon budget (e.g., $> 1$ GtC). A recent global study provides improved estimates of seaweed cultivation and carbon sequestration potential[31], but it is limited to one seaweed group and does not elaborate on uncertainties. Here we develop and use a global dynamic model of seaweed growth, the Global MacroAlgae Cultivation MODelling System (G-MACMODS), to analyze the potential of seaweed farming to produce Gt-scale biomass carbon under the assumptions of bottom-up limitation mechanisms. We focus on the cultivation of four seaweed types and systematically test the sensitivity of seaweed production to a range of uncertain biophysical parameters.

Details of G-MACMODS, data sources, and analytical methods are in *Methods*. In summary, the model[32](Supplementary Fig. 1) predicts spatially-resolved (1/12th$^\circ$ resolution) seaweed cultivation with constraints from both extrinsic (environmental

forcing) and intrinsic factors (biological parameters; e.g., growth rates, nutrient uptake and storage, exudation, and mortality, among others). To test sensitivities and evaluate uncertainties, we performed $\sim$ 800 simulations of global growth and harvest for four seaweed types (using biophysical characteristics based on currently-farmed temperate and tropical red and brown genera). Each simulation sampled from a uniform distribution of parameter values spanning the full range of relevant values reported in the literature (Table 1), and was forced with temperature, solar irradiance, current velocities, wave height, wave period, and nutrient data sourced from a combination of satellite measurements (MODIS) and global ocean model simulations (HYCOM and CESM). Although we tested the model with forcing data from different years, results reported here reflect the year 2017 (a recent year without strong El Niño/La Niña anomalies; Supplementary Figs. 2-3), and a seasonally-variant climatology of nutrient inputs (Supplementary Fig. 4). Simulations that use parameter values best supported by literature are termed "standard runs." Seeding and harvesting for each seaweed type were optimized based on the standard runs. We also assess the importance of different model parameters via Monte Carlo methods and “random forest” classification analysis.

G-MACMODS assumes nitrogen is the limiting nutrient (i.e. implying that micronutrient constraints could be overcome by farming practices). The 800 simulations of each seaweed type were split between two bounding nutrient scenarios: (1) an "ambient nutrient" case in which average nitrate concentrations within the top 20 m are available to seaweed without depletion or competition, and (2) a "flux-limited" case where only the mass of nitrate replenished through vertical flux across 100-m depth is available to seaweed. The ambient scenario, while unrealistically optimistic for intensive production on a global scale without artificial upwelling, is illustrative of farming at a scale that does not generate substantial feedback modifying regional nutrient budgets. In contrast, the flux-limited scenario may better reflect nutrients in a situation of dense farming or nutrient competition from phytoplankton[31,33]. However, both are idealized scenarios because the “offline” implementation of G-MACMODS cannot explicitly account for feedback to nutrient cycling; the different scenarios are intended to help gauge the sensitivity of seaweed production to nutrient constraints. Our analysis focuses on offshore production, as competing uses and poor resolution of coastal nutrient inputs limit model fidelity in the nearshore. The purpose of this work is not to advocate for the widespread deployment of seaweed farms over a significant fraction of the global oceans, as we expect this would come with unacceptable trade-offs to ocean health, but rather to assess the geographic distribution and potential of offshore seaweed farming to produce biomass at climate-relevant scales.

## Global Seaweed Yields

Maps in Figure 1 show the magnitude and types of seaweed harvested in our standard simulations of the ambient and flux-limited nutrient scenarios (where the seaweed type that produces the largest harvest in each grid cell is farmed). Seaweed could be harvested over large areas of the ocean (208 million km$^2$ and 132 million km$^2$ in the ambient and flux-limited runs, respectively; cf. 6, 31); however, yields vary substantially in space, and annual harvests are vastly different in the two nutrient scenarios. The most productive locations include the equatorial Pacific and upwelling regions (e.g., along coasts or near energetic western boundary currents). Almost no seaweed is harvested in either nutrient scenario in the oligotrophic regimes characteristic of the center of the subtropical oceanic gyres (Figs. 1b and 1c).

Although G-MACMODS does not dynamically represent the interaction between farmed seaweed and phytoplankton, we compare the modeled rates of carbon fixation by seaweed (seaweed net primary productivity (NPP)) with phytoplankton NPP estimated from satellite ocean-color observations[34] (Fig. 1a and Figure 1d). While phytoplankton NPP includes a significant component fueled by recycled nutrients in the euphotic zone, it represents an upper bound on new production or, similarly, net community production (NCP; typically, $\sim$ 10-20 % of phytoplankton NPP[35]). Seaweed have average carbon-to-nitrogen ratios (C:N) of $\sim$ 20:1 in temperate regions[36,37] and $\sim$ 40:1 in tropical regions[38–40], which are much higher than the $\sim$ 6.6:1 (Redfield ratio) typical of phytoplankton. For the same amount of nitrogen, therefore, seaweed can fix 3-6 times as much carbon. However, in our ambient nutrient simulations, seaweed NPP is 7 and 14 times larger than observed phytoplankton NPP ($\sim$ 35 and 70 times larger than phytoplankton NCP) near the temperate and tropical regions, respectively, implying that the modeled seaweed growth consumes more than 10 times the nitrogen that is taken up by phytoplankton NCP (Fig. 1a). This suggests that the ambient nutrient case does not provide a sound basis for estimating potential productivity of widespread, intensive farming in the absence of artificial upwelling, but it might provide a reasonable estimate of the potential harvests of operations small enough in scale so as to not radically alter local nutrient budgets. Indeed, the yields simulated in the ambient nutrient scenario results agree well with harvest values reported in the literature for many small farms and a few large farms situated near nutrient outflows (Supplementary Figs. 5-8). In contrast, zonally-averaged seaweed NPP is less than observed phytoplankton NPP in our flux-limited simulations, except in equatorial regions where phytoplankton growth is iron-limited[41,42] (Fig. 1d), consistent with our NCP constraint. The lower harvests estimated in the flux-limited scenario may therefore better reflect production when farming at scales large enough to significantly deplete the surface fixed-nitrogen inventory, relying on the influx of "new"

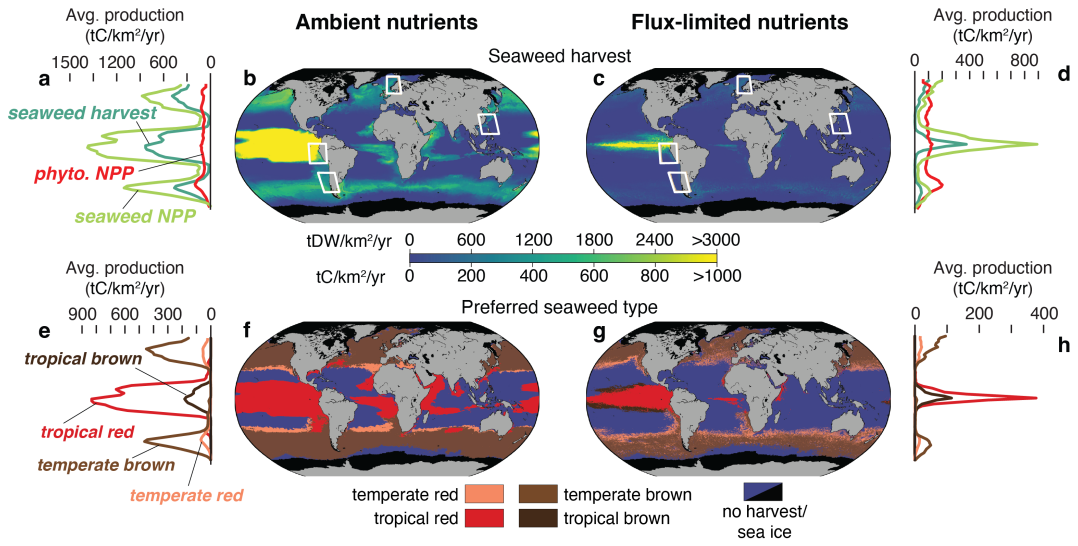


**Figure 1. Global seaweed harvest.** Maps of annual potential harvest per unit area (yield; b-c) of the preferred seaweed (the type with the largest harvest in each grid cell; f-g). White boxes correspond to regions depicted in Figure 2. Zonally-averaged annual harvest for the preferred seaweed group, seaweed net primary productivity (NPP), and phytoplankton NPP estimated from satellite observations[34] are shown in (a,d). Zonally-averaged annual harvests for the four seaweed types are shown in (e,h).

nitrogen from below the nutricline (Figs. 1c and 1d).

The standard simulations of both nutrient scenarios predict that temperate brown and tropical red seaweed out-compete temperate red and tropical brown seaweeds over most of the global ocean. When nutrients are abundant, temperate red seaweed appear at the equatorward edges of regions with temperate brown seaweed (Figs. 1f and 1g). The zonally-integrated annual harvest of tropical red seaweed is 3-4 times higher than that for tropical brown seaweed; similarly, the zonally-integrated annual harvest of temperate brown seaweed is 4-8 times larger than that for the temperate reds (Figs. 1e and 1h).

At regional scales (e.g., areas enclosed by boxes in Figures 1b and 1c), physical processes such as western-boundary current meanders (Fig. 2a), coastal upwelling (Fig. 2l), and frequent eddy activity (Fig. 2k) influence environmental variability and seaweed growth. Four factors govern seaweed growth rate in the model: water temperature, nutrient availability, light, and seaweed density, or "crowding"(equation 7). Of these factors, water temperature largely determines the latitudinal distribution of different seaweed types (e.g. tropical seaweeds in the South/East China Sea (Fig. 2, top row) and temperate seaweed in the Norwegian Sea (Fig. 2, third row)). At smaller scales, nutrient availability controls regional patterns of seaweed productivity and, as expected, is more important in flux-limited simulations than in the ambient nutrient scenario (Fig. 2). Light availability and crowding (e.g. self-shading, sub-grid scale nutrient competition) can become relatively important growth limitation factors in regions with readily available nutrients.

## Uncertainty Analysis

We assess the sensitivity of our results to uncertainty in the biophysical parameters in G-MACMODS, conducting a Monte Carlo analysis over a range of literature-based parameter values with uniform distribution (Table 1). The standard deviation of Monte Carlo simulations increases in direct proportion to the simulated harvest yield (Fig. 3). For example, regions with larger harvests in our standard simulations also show greater variability in the Monte Carlo results (Figs. 3e and 3f; Figures 3a and 3b as compared to maps in Figures 1b and 1c). In the most productive 10% of the regions of the ocean, the average yield can range 646–1589 GtC/km$^2$.

Based on a random forest analysis of Monte Carlo results, the biological parameters that most influence harvested seaweed yield globally are the mortality rate and nitrogen exudation rate (Figs. 3g and 3h). Our Monte Carlo simulations evaluate mortality rates from 0.003/day - 0.017/day; some prior models have used similar or slightly lower values (0.001/day - 0.01 /day)[28,29,43,44]. Nitrogen exudation rates are more important in determining harvest in the flux-limited simulations than in the ambient scenario, since exudation (i.e., slimy excretion from the seaweed) leads to loss of nutrients that are already scarce in the

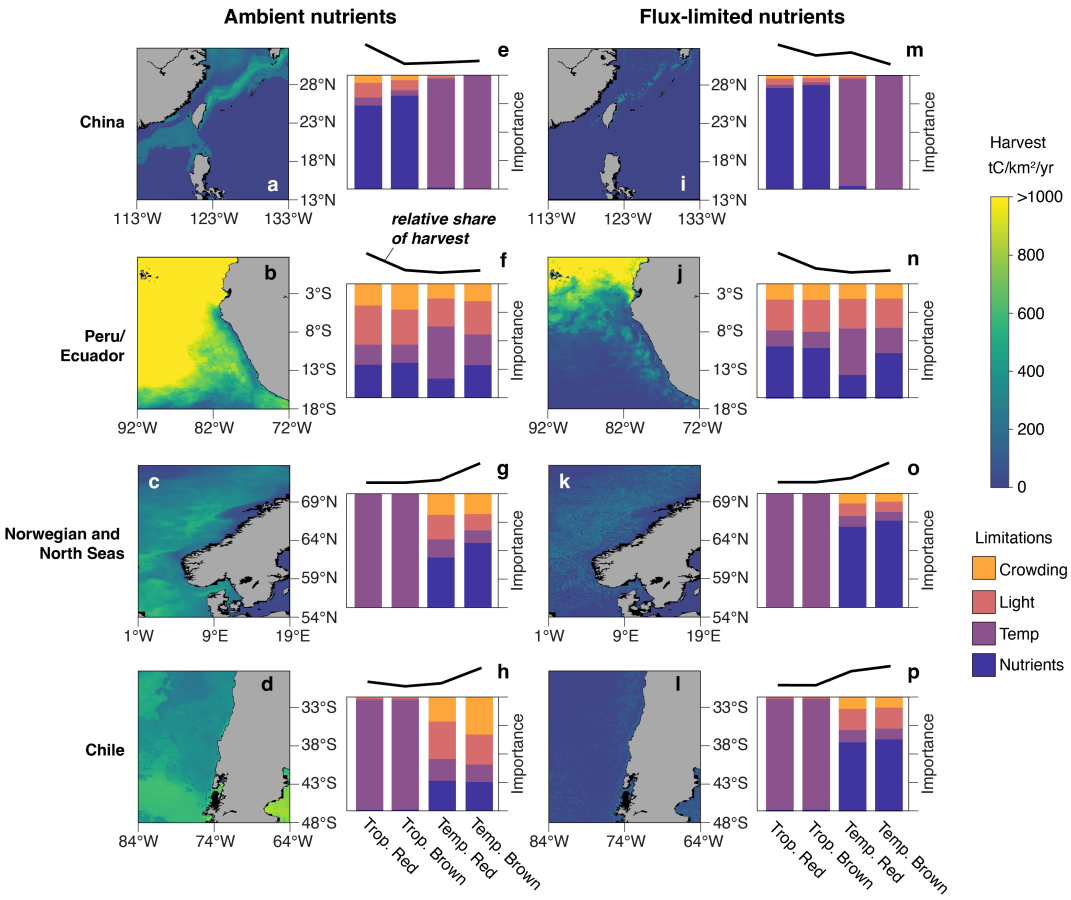


**Figure 2. Regional harvest.** (Maps a-d, i-l) Annual harvest yields for the boxed regions in Figure 1. (Bars e-h, m-p) Relative influence of growth parameters (equation 7) in determining regional harvest yield for each seaweed type. (Spark lines) Relative spatially integrated annual harvest for each seaweed type.

flux-limited case. The value of the maximum growth rate also heavily influences harvest estimates in less productive regions. Since seaweed is only harvested once it reaches a target weight (see *Methods*), the maximum growth rate influences whether and how quickly the seaweed reaches a harvestable condition. Among the other biological parameters, nitrate uptake kinetic parameters ($V_{max}$, $K_s$, B:SA) play a relatively important role when nutrients are abundant (Fig. 3g), and the value ascribed to the minimum nitrogen cell quota ($Q_{min}$) becomes important when nutrients are difficult to attain (Supplementary Fig. 9).

## Scaling production in EEZs

The maps in Figure 4 show the area of exclusive economic zones (EEZs) that would be required to grow seaweed biomass of 1, 2, and 4 GtC/year in our standard, flux-limited simulation. Cumulative distributions of seaweed-based annual harvest in the standard, flux-limited simulation as a function of EEZ area (sorted by harvest yield, such that the areas with the largest harvests are cultivated first; Figure 4e) show diminishing returns from farming more than $\sim$ 15% of EEZs (locations scattered across the world), with harvests approaching a limit of $\sim$ 4.5 GtC/year at $\sim$ 25% of EEZs (Fig. 4e). In the standard, flux-limited simulation, 1 GtC/year could be harvested from the most productive $\sim$ 0.8% of EEZs (1 million km$^2$; located in the equatorial Pacific; Figure 4a), ranging from 0.36 to 1.8 GtC/year at the 5th to 95th percentiles of flux-limited Monte Carlo simulations but always less than the 2.4 GtC/year yield predicted in the standard, ambient nutrient simulation (Fig. 4f).

# Implications for seaweed CDR

This work represents an advance over previous estimates in that it employs a mechanistic seaweed growth model (G-MACMODS) to dynamically simulate four types of seaweed under two bounding nutrient scenarios and evaluates parametric sensitivities; it is an important first step towards a fully prognostic model. The standard simulation model results have been

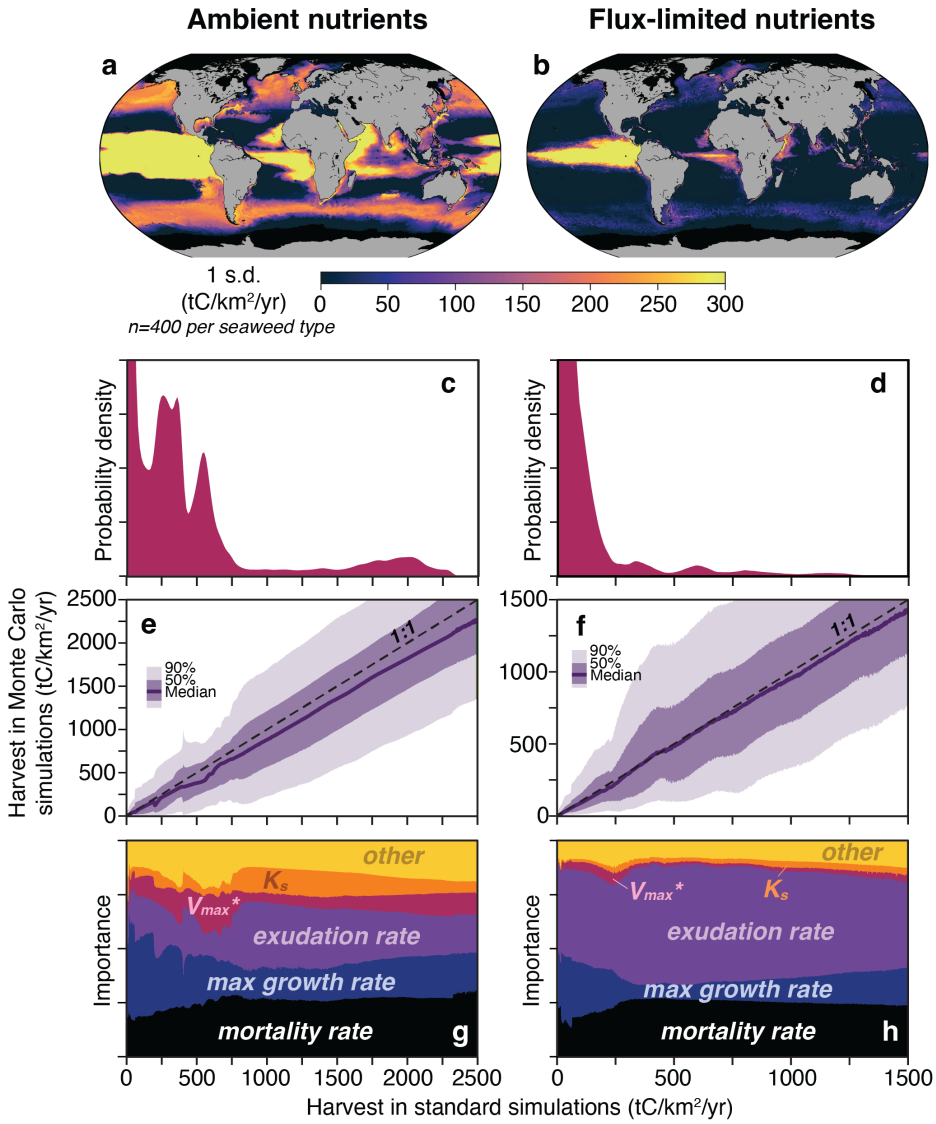


**Figure 3. Harvest uncertainty.** Maps of standard deviation from the Monte Carlo results (a,b) and probability density function (PDF) of the standard run annual harvest yield (c,d). The y-axis has been cut off to better visualize the smaller PDF values (corresponding to larger harvests). Bin-averages of Monte Carlo statistics are shown as a function of the standard run results (e,f). The median harvest is shown as a solid line; the dark and light shading denote the values between the 25th and 75th percentiles and the 5th and 95th percentiles, respectively. The dashed 1:1 line shows where the median harvest would lie if it equaled the standard harvest. The relative importance of the biological parameters in Table 1, as quantified by random forest analysis, are depicted in (g,h). $V^*_{max}$ [$\mu$mol-N/(m$^2$ h)] is the product of the maximum uptake rate ($V_{max}$) and the ratio of biomass-to-surface area (B:SA). The biological parameters not explicitly named are grouped under the "other" category (Supplementary Fig. 9).

evaluated in comparison to available and relevant published values of farmed and wild seaweed yield (Supplementary Figs. 5-8). The ambient nutrient scenario, which assumes that nutrient levels are unaffected by seaweed farms, represents a global extrapolation of current-scale, coastal seaweed farming. But it is not clear that depleted nutrients could be replaced through transport from the surrounding environment without quickly straining the inventory of global nutrients and disrupting the natural biological carbon pump[31]. Sustaining levels of production in ambient simulations over large areas would thus require some form of nutrient amendments (e.g. artificial upwelling), which would, in turn, entail additional costs. Our flux-limited nutrient simulations instead reflect offshore seaweed production that might be sustainable given local resources by using only "new" nitrogen replenished from the deep ocean (fluxed upward across the 100 m depth). Relative to the ambient scenario, the standard flux-limited simulations reduce potential seaweed harvest worldwide by an average 90%.

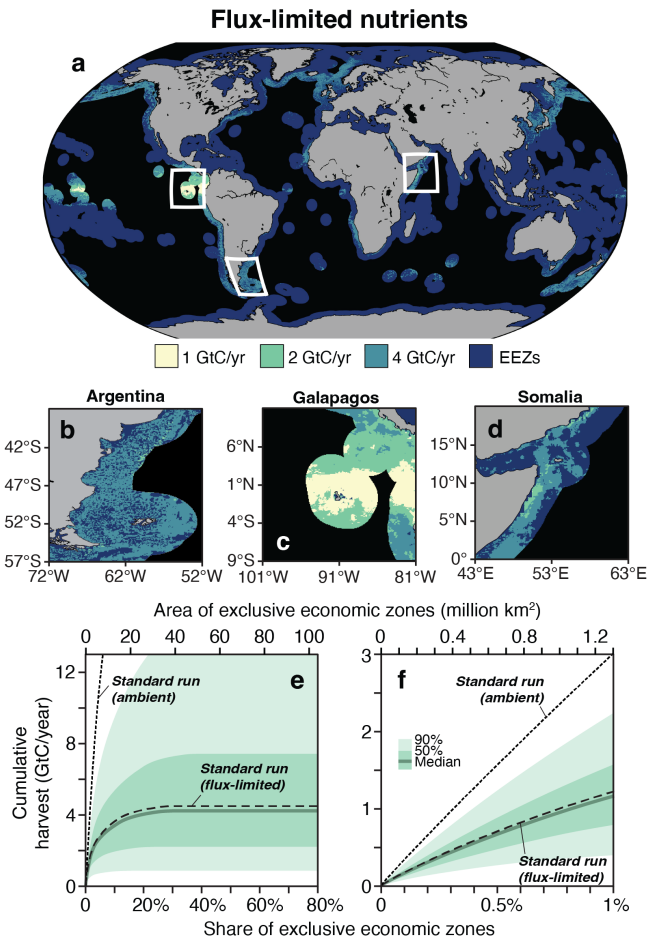


**Figure 4. Total potential harvest in EEZs.** (a-d) Areas of exclusive economic zones (EEZs) required to harvest 1, 2, and 4 GtC/year of seaweed biomass in standard, flux-limited simulations, sorted by productivity (i.e. prioritizing the most productive areas). (e-f) Cumulative distribution functions of total seaweed carbon harvested relative to the share of global EEZs farmed. Results from the ambient and flux-limited standard runs are depicted as dashed lines. The solid green line and surrounding shading indicate the range of harvests of Monte Carlo, flux-limited simulations.

Even in flux-limited simulations, though, we estimate that a climate-relevant mass of carbon (e.g., 1 GtC) might be harvested by farming seaweed in the most productive 0.8% of EEZs (Fig. 4f). However, 0.8% of EEZs worldwide ($\sim$ 1 million km$^2$) would represent a roughly 370-fold increase in the area where seaweed is currently farmed ($\sim$2700 km$^2$[18,45]). For comparison, the area occupied by all agricultural cropland in the U.S. is $\sim$1.6 million km$^2$[46]. The National Academy of Sciences suggests that if seaweed cultivation comprises one of several CDR strategies, this industry would only need to extract $\sim$ 0.03 GtC/year[5]; however, even this target requires increasing the current seaweed cultivation area by over 10-fold and moving it to the most productive regions of the ocean. While conversations center on seaweed harvest yield, the harvested biomass accounts for an average 45% of the total seaweed biomass produced in our standard runs; the remaining 55% is grazed, remineralized, buried *in situ*, or exported from the farm as particulate organic carbon. Of the seaweed carbon that is not harvested, if 1% and 2% is buried in the shelf or exported to the deep sea, respectively (as estimated for wild seaweed[25]), then for every 1 GtC harvested from farms over the continental shelf, 0.02 GtC could be buried, and 0.03 GtC could be exported to the deep sea. However, carbon removed from the atmosphere may be less than harvested carbon due to time scales of air-sea carbon fluxes and disruptions to the natural biological carbon pump[31,47].

As indicated by the variance among Monte Carlo simulations, the largest uncertainties in our estimates of seaweed harvest correspond to mortality and exudation rates. The mortality rate in the model reflects erosion, dislodgement, pests, herbivory, diseases, sedimentation, and natural disasters. Our standard simulations assume a mortality rate of 1% per day (Table 1).

Existing models and observations span both lower[28,29,31,44,48] and higher mortality rates[36,49,50], yet these sources, which primarily consider nearshore farms, may have limited applicability to mortality on open ocean farms. Like mortality, nitrogen exudation by seaweeds is understudied, despite its importance in modeling productivity in nutrient-limited waters. Nitrogen exudation rates between 0.002/day[36] and 0.2/day[51] have been reported. We assume a constant rate of nitrogen exudation (0.05/day in the standard simulations), but the rate is likely to fluctuate in time with environmental conditions[52–54] and ratios of nutrients in the seaweed (as observed for carbon exudation)[54–57]. Although not represented in our model, exudation rates may be related to seaweed growth rates[51], and mortality rates[58]. Maximum growth rate, maximum uptake rate, and half saturation constant also affect estimated harvests to varying but lesser degrees (Fig. 3). Maximum growth rate cannot be easily parsed from observations of relative growth rate, and existing maximum uptake rate and half saturation constants may not have been estimated using standardize environmental conditions. Our results thus highlight the importance of further research to narrow uncertainties related to mortality and exudation rates under real-world conditions expected during cultivation and thereby narrow the uncertainty bounds around our harvest estimates.

Despite the limitations of our model and substantial uncertainties related to biophysical parameters, we estimate the global potential for seaweed farming in unprecedented detail. Our results suggest that it may be possible to annually harvest seaweed containing 1 GtC/year by farming on the order of 1 million km$^2$ of the most productive ocean areas. However, in addition to narrowing uncertainties and accounting for the effects of climate change, future work must further assess the economic and political feasibility of farming seaweed over such large areas that may have other uses or protections (e.g., fishing, shipping traffic, marine protected areas). Similarly, if the purpose of harvesting such large quantities of seaweed is to sink it to the deep ocean and thereby sequester carbon, the effects on abyssal ecosystems[59–61] and possibility of increasing the extent of hypoxic regions[62,63] deserve more investigation. But although there remain many unknowns and hurdles for large-scale seaweed farming, our analysis suggests that harvesting quantities of seaweed that would make a substantial contribution to global CDR is possible and future investment in research is warranted.

# Online Methods

## G-MACMODS Overview

The Global Macroalgae Cultivation Modelling System (G-MACMODS) used in this study draws on recent work on within-farm biophysics[32], using elements from previously published research[26–28]. The state variables in the model are seaweed biomass (B; g-DW/m$^2$; where DW is dry-weight) and nitrogen cell quota (Q; mg-N/g-DW;[64]). Nitrogen is the limiting macronutrient in G-MACMODS. Though we recognize that other macronutrients and micronutrients could further limit our results in, for example, high-nitrogen low chlorophyll environments[42], we assume that the aquaculture industry has implemented micronutrient fertilization. G-MACMODS estimates seaweed biomass in units of dry weight; biomass is converted to units of carbon by assuming that carbon constitutes 30% of the seaweed dry weight for all seaweed groups[65,66], though carbon content may actually be lower for tropical red seaweed[39].

A diagram of the conceptual model is presented in Supplementary Figure 1. The model has a daily time step and considers macroalgae to be grown at 2 m depth below the surface for the purposes of light attenuation. Seaweed biomass is depth-integrated across the top 20 m of the water column.

## Model structure

Temporal changes in the state variables ($B$ and $Q$) can be described with the following equations:

$$\frac{dQ}{dt} = V - \mu(Q - Q_{min}) - E(Q - Q_{min}), \tag{1}$$

and

$$\frac{dB}{dt} = \mu B - d_M B, \tag{2}$$

where $V$ is the nitrogen uptake rate [$\mu$mol-N/(g-DW h)], $E$ is a fractional exudation rate (1/day), $\mu$ is the fractional growth rate (1/day), and $d_M$ is the fractional death rate (1/day).

### Nitrogen Uptake

The rate of nitrogen uptake by seaweed is determined by extrinsic (environmental) and intrinsic(biological) limiting factors:

$$V = V_{max}\, f(Q)\, f(|\vec{v}|, T_w, C), \tag{3}$$

where $V_{max}$ is the maximum uptake rate (Table 1), $f(Q)$ represents a dynamic nutrient cell quota which allows for luxury uptake of nutrients, and $f(|\vec{v}|, T_w, C)$ represents both kinetic and mass-transfer limitations on nitrogen uptake. We use a linear nutrient cell quota[32]:

$$f(Q) = \frac{Q_{max} - Q}{Q_{max} - Q_{min}}, \tag{4}$$

where $Q_{min}$ is the minimum amount of nitrogen that should be found in a seaweed cell (structural nitrogen), $Q_{max}$ is the maximum amount of nitrogen stored internally, such that uptake decreases as the internal nitrogen concentration increases, and $f(Q)$ is a unitless coefficient between 0 and 1. The parameter $f(|\vec{v}|, T_w, C)$ in equation (3) is a limit on uptake based on a combination of Michaelis-Menten kinetics and mass-transfer limitation regulated by the surrounding waves and currents[67–69] :

$$f(|\vec{v}|, T_w, C) = \frac{C}{K_m\left(\frac{C}{K_m} + \frac{1}{2}\left(\gamma + \sqrt{\gamma^2 + 4\frac{C}{K_m}}\right)\right)}, \tag{5}$$

where $\gamma = 1 + (V_{max}/\beta K_m) - (C/K_m)$, $K_m$ is the half-saturation constant (Table 1), $C$ is the external concentration of nitrogen, and

$$\beta = \frac{D}{\delta_D} + \frac{4\delta_D}{T_w}\sum_{n=1}^{\infty}\left(\frac{1 - \exp\left(\frac{-Dn^2\pi^2 T_w}{2\delta_D^2}\right)}{n^2\pi^2}\right) \tag{6}$$

with units of m/s. In equation (6), $D$ is the molecular diffusivity of nitrate at 18° C (7.3 × $10^{-10}$ $m^2$/s)[32,70], $T_w$ is wave period, and $\delta_D$ is the thickness of the diffusive boundary layer, defined using the thickness of the viscous boundary layer $\delta_D = \delta_\nu = 10\nu/(\sqrt{C_D}|\vec{v}|)$ where $\nu$ is the molecular kinematic viscosity ($10^{-6}$ $m^2$/s) and $C_D$ is the drag coefficient[69] (Table 1). The parameter $f(|\vec{v}|, T_w, C)$ is unitless and varies between 0 and 1. Note that this nitrogen uptake model assumes that (a) the diffusion boundary layer is completely stripped away every half a wave period, regardless of the size of the wave, (b) the thickness of the diffusive boundary layer ($\delta_D$) can be parameterized with the thickness of the viscous boundary layer ($\delta_\nu$), and (c) that we can ignore near-boundary turbulent transport (i.e. assume the blade is smooth)[69], though this has been shown to enhance exchange rates[71]. We do not consider within-canopy flow reduction, which negatively affects uptake[32,72]. We assume that wave height has a negligible affect on uptake, since renewal of the diffusive boundary layer (and, hence, enhanced nutrient uptake) can occur through blade flapping in low-flow environment[73]. Thus, equation (3) is used to estimate the amount of nitrogen that the seaweed could, theoretically, absorb from the environment ($dN$).

Two nutrient scenarios are tested in this study: (1) a case where nutrient concentrations are averaged over the top 20 m of each grid cell and are available to seaweed without depletion or competition is referred to as the "ambient nutrient" scenario, and (2) a case where the amount of nutrients available for uptake is capped by the nitrogen fluxed upward through the 100-m depth plane ($N_{new}$), referred to as the "flux-limited" scenario. In the flux-limited scenario, the nitrogen uptake rate (equation 3) is still determined by the "ambient" (average of top 20 m) nutrient concentration, but if the amount of nitrogen that would be theoretically taken up by seaweed at a given time is greater than that fluxed upward at 100 m depth, $dN > N_{new}$, then uptake ($V$ in equation 1) is capped using $dN = N_{new}$. Additional simulations were performed to test an alternate depth for estimating $N_{new}$ - at the annual maximum mixed-layer depth at each grid cell - but resulting productivity differences were relatively small compared to other uncertainties presented in the *Uncertainty Analysis* section (median increase of 5% in the annual harvest yield).

### Growth

Similar to the nitrogen uptake rate, growth rate ($\mu$) is also constrained by extrinsic and intrinsic limiting factors:

$$\mu = \mu g(k)\, g(Q)\, g(T)\, g(E), \tag{7}$$

where $\mu g(k)$ (1/day) is the maximum growth rate at a given seaweed density, accounting for the crowding effects of self-shading and within-farm (sub-gridscale) nutrient limitation. The maximum growth rate is further constrained by the internal nitrogen cell quota $g(Q)$, water temperature $g(T)$, and light $g(E)$, all of which are unitless coefficients, varying between 0 and 1.

The growth rate limitation imposed by crowding in the seaweed canopy embodies the general idea that less-dense seaweed can grow faster, described as

$$\mu g(k) = A\, B^{-0.75}, \tag{8}$$

where $A$ [(1/d)/(g-DW/m)] is a factor that represents the growth rate at the maximum allowable biomass density. Strictly defined, $A = k_R/B_{cap}^{-0.75}$, where $B_{cap}$ (g-DW/m) is the maximum biomass density and $k_R$ is the maximum growth rate at $B_{cap}$ [chosen to be 5% per day and tuned to match values documented in the literature for our different seaweed types (Supplementary Figs. 5 - 8)].The power law in equation (8) was derived by re-fitting data from a comprehensive meta analysis[74]. Our new fit was applied over the data in ref. 15 and binned to 0.01-width bins from 0–1 g/L and 0.1-width bins for 1–60 g/L seaweed density, weighted by the number of observations in each bin (with a minimum weight of 8 observations). Our fit excluded data corresponding to total-nitrogen ($NO_3$+$NH_4$) conditions not likely to be found in the surface ocean (values above 20 $\mu$M). Although according to equation (8), $\mu g(k) \to \infty$ as $B \to 0$, we cap the maximum growth rate ($\mu_{max}$) according to values found in the literature (Table 1), such that $\mu g(k) \to \mu_{max}$ as $B \to B_{seed}$, where $B_{seed}$ is the seed weight.

The nitrogen quota limitation $g(Q)$ in equation (7) follows the Droop model[64]:

$$g(Q) = \frac{Q - Q_{min}}{Q}. \tag{9}$$

where $Q_{min}$ is set per species type (Table 1). The temperature limitation term in Equation (7) is similar to a Gaussian probability curve[75]:

$$\begin{aligned} g(T) &= \exp\left(-\beta_1 (T - T_{opt})^2\right), T < T_{opt} \\ g(T) &= \exp\left(-\beta_2 (T - T_{opt})^2\right), T > T_{opt} \\ g(T) &= 1, T = T_{opt}, \end{aligned} \tag{10}$$

where $T_{opt}$ is a 5° optimal temperature range for each seaweed group that we are examining, $T$ is the daily temperature, and the $\beta_1$ and $\beta_2$ coefficients are adjusted to reach zero near the lower and upper temperature limits, respectively.

The light-limitation in equation (7) is largely informed by phytoplankton studies[76]:

$$g(E) = f \frac{I - I_c}{I_s - I_c} \exp\left(-\frac{I - I_c}{I_s - I_c} + 1\right), \tag{11}$$

where $I_s$ and $I_c$ are the daily-averaged saturating and compensating irradiance (W/m$^2$), $f$ is the fraction of daylight that is implemented to account for periods of darkness, and $I$ is the irradiance reaching an underwater depth of 2 m. The irradiance is attenuated following the implementation in the Marine Biogeochemistry Library (MRBL)[77,78].

***Mortality***

The mortality rate, $d_M$ in equation (2), is the sum of a constant daily mortality rate that is meant to incorporate grazing, aging, and disease ($d$; Table 1) and a term that accounts for breakage from waves ($d_w$), such that $d_M = d + d_w$. The $d_w$ term is dependent on wave power and, as such, is variable in both time and space[79]:

$$d_w = (2.3 \times 10^{-4})(P \times 10^3) + 2.2 \times 10^{-3}, \tag{12}$$

where $P$ is wave power in Watts:

$$P = \frac{\rho g^2}{64\pi} H_s^2 T_w \tag{13}$$

where $\rho$ is the density, $H_s$ is the significant wave height, and $T_w$ is the wave period.

## Environmental data

The environmental inputs applied to our model (water temperature, solar irradiance, current velocities, wave height, wave period, and nutrient concentrations) stem from a combination of satellite measurements and global ocean model outputs spanning multiple years. For the purposes of this manuscript, we explore a suite of simulations using inputs from 2017, the most recent year with available data that is also not identified with having a strong ENSO index. Input data from 2003-2019 were using in simulations examining inter-annual differences in estimated seaweed productivity (Supplementary Fig. 10), however, regional inter-annual variability was comparatively small with respect to parameter uncertainty and is therefore not the focus of this study.

Sea surface temperature (SST) and surface photosynthetically active radiation (PAR) are used as a proxy for $in-situ$ temperature and irradiance, respectively, over the depth of macroalgae growth. SST and PAR used in this study are 8-day averages from the MODerate Resolution Imaging Spectroradiometer (MODIS; R2018), on the NASA Earth Observing System, with spatial resolution of 1/12°. Net oceanic primary production (NPP) was estimated from MODIS chlorophyll measurements using the Vertically Generalized Production Model (VGPM)[34]. SST, PAR, and NPP were downloaded from the Ocean Productivity website (https://sites.science.oregonstate.edu/ocean.productivity/index.php).

Zonal and meridional current velocities were extracted from the HYbrid-Coordinate Ocean Model (HYCOM[80]) Global Ocean Forecasting System (GOFS) 3.1, accessed from https://www.hycom.org/dataserver/gofs-3pt1/analysis. HYCOM is a global data-assimilating model[81] with 1/12° horizontal resolution and 41 depth levels, of which we use the surface velocities.

Significant wave height and wave period were taken from the European Centre for Medium-Range Weather Forecasts (ECMWF) ERA5[82] atmospheric reanalysis produced by the Copernicus Climate Change Service[83]. ERA5 provides hourly significant wave height of combined wind waves and swell, and mean wave period with a 1/2° horizontal resolution. The data are averaged to 8-day time intervals.

Nutrient information is taken from a high resolution biogeochemical simulation led by the National Center for Atmospheric Research (NCAR) and run in the Community Earth System Model (CESM) framework[84,85]. The biogeochemical model has a 1/10th ° horizontal resolution and 62 depth levels. Fields used in this study include 5-day mean nitrate concentrations averaged over the upper 20 meters, and vertical fluxes of nitrate across the 100-m depth plane were calculated to provide and estimate of fluxes of new nitrogen into the euphotic zone. All 5-day outputs were interpolated to 8-day periods for consistency with the other environmental inputs to G-MACMODS.

Although G-MACMODS steps forward with a daily time step, we apply the 8-day environmental inputs that best correspond to the G-MACMODS time stamp. All environmental inputs were spatially interpolated onto a 1/12 ° global grid, using linear interpolation if the input data were of higher resolution, or nearest-neighbor if the input data were of lower resolution.

## Seaweed groups

Here, we focus on four seaweed groups containing seaweed species that are among the world's ten most cultivated by weight[86]: tropical reds (e.g. *Eucheuma, Gracilaria, Kappaphycus*), tropical browns (e.g. *Sargassum*), temperate reds (e.g. *Porphyra*), and temperate browns (e.g. *Saccharina, Laminaria, Macrocystis*). Values of parameters required by G-MACMODS were gathered from available literature for a few representative seaweed genera (Table 1); "standard runs" were defined using average (when multiple parameter estimates were available) or speculated values (based on information from other genera when there were few or no published values). We define the temperature parameters in equation 6 similarly, using available information for representative genera (Table 2). The optimal temperature range in equation 6 is extended to a 5° width, rather than a single number, to account for variations within a seaweed genus.

The standard runs were spun up for one year, and the seeding was optimized by choosing the run initialization date that yielded the largest yearly biomass harvest (averaged across 2003-2019) for every grid point. Tropical and temperate brown

seaweed runs were seeded with 50 g-DW/m$^2$. Tropical and temperate red seaweed runs were seeded with 200 g-DW/m$^2$ and 10 g-DW/m$^2$, respectively, following examples in the literature (see references in Supplementary Figs. 5-8). Seaweed are seeded with an initial nitrogen cell quota ($Q_0$), such that

$$Q_0 = Q_{min} + \frac{N}{35}\left(Q_{max} - Q_{min}\right), \tag{14}$$

where N/35 is the ratio of the ambient nitrogen concentration at the time of seeding to the a representative N concentration below the nutricline (35 $\mu$M).

## Model-Field Data Comparison

To test our choice of standard parameters (Table 1) and calibrate $B_{cap}$ and $k_R$ (equation 8), harvested yield from our standard runs was compared to literature values of harvested yield that encompass ocean-cultivated and wild seaweed stocks. Only farmed values published after the year 2000 are included to account for changes in technology and methods across the years, whereas we include wild stock values from literature published as far back as 1990.

To test our model performance around tropical red seaweed, we executed ambient runs with a 45-day harvest period (standard in literature; e.g. 87–92) and compared the maximum amount of biomass harvested at every grid cell within a single harvest period to *Eucheuma* and *Kappaphycus* harvest yields in the literature (Supplementary Fig. 5). The median harvest yield in G-MACMODS is larger than the median harvest yield reported in the literature, but the 50% range surrounding the medians is comparable. Our model never reaches some of the larger harvest values in the literature, but we attribute that to the difference in farming depths; eucheumoids are typically farmed in depths shallower than 10 m, often very close to shore where terrestrial nutrient inputs may be significant, whereas our model considers nutrients depth-averages over the top 20 m of the water column.

G-MACMODS performance for tropical browns, temperate reds, and temperate browns was tested without including harvest, comparing the maximum seaweed biomass per grid cell in our ambient runs to the maximum biomass per unit area harvested on a seaweed plot or observed standing stock (Supplementary Figs. 6-8). All median harvest yields from G-MACMODS surpass the median harvest yields in the literature, suggesting that the G-MACMODS results are optimistic.

## Harvest

Harvest schemes were based on available information of current farming practices (e.g. 19, 31, 91–95) and optimized for each seaweed group to achieve maximal biomass per harvest based on standard run tests of three harvest schemes: periodic harvesting, periodic harvesting with a biomass threshold, and conditional harvesting (with a dual criteria of a target weight or when death exceeds growth). The test runs also allowed for optimization of the target weight to initiate harvest (10 %, 20 %, 30 %, 40 %, 50 %, or 80 % of $B_{cap}$), as well as the percent of biomass removed at each harvest (40 %, 60 %, or 80 % ). Finally, the number of harvests per year were limited based on documented cultivation practices. The temperate brown and red alga are commonly harvested twice[19] and 6 times a year[93], respectively, while the tropical brown and red alga are harvested up to 8 times a year[92,96]. Temperate brown seaweeds were allowed to grow without consideration for harvest for at least 60 days after seeding. Considering the above factors, the harvesting schemes that produced the highest harvested yields for each seaweed group are as follows:

1. Tropical red and brown seaweeds: Harvest occurs every 45 days only if the seaweed biomass has reached the target weight of 800 g-DW/m$^2$ (27 % of $B_{cap}$) for tropical reds and 400 g-DW/m$^2$ (50 % of $B_{cap}$) for tropical browns. If 45 days elapse and the seaweed does not reach its target weight, another 45-day period must transpire before re-evaluating the biomass. If the biomass has reached its target weight, then 80 % of the biomass is harvested.

2. Temperate red seaweeds: Harvest is initiated whenever the biomass reaches the target weight (80 g-DW/m$^2$, 40 % of the $B_{cap}$) within 150 days after seeding or if the death exceeds growth for 7 days. If the biomass has reached its target weight then 80 % of the biomass is harvested; if the death exceeded growth for > 7 days or the final harvest period is reached, 99 % of the biomass is harvested (1 % loss rate assumed in final total harvest).

3. Temperate brown seaweeds: Harvest occurs when the biomass reaches the target weight (1350 g-DW/m$^2$, 68 % of the $B_{cap}$) within 220 days after seeding or if death exceeds growth for 7 days. If the biomass has reached its target weight, then 80 % of the biomass is harvested; if the death exceeded growth for > 7 days or the end of 220 days is reached, 99 % of the biomass is harvested (1 % loss rate assumed in final total harvest).

## Monte Carlo simulations

We used Monte Carlo methods to estimate the uncertainty surrounding our standard run harvest amounts. We performed between 425 - 450 Monte Carlo simulations for each seaweed group and nutrient scenario (ambient vs. flux-limited). Each Monte Carlo simulation chose the value of the seaweed biological parameters using a uniform probability distribution bounded by the magnitudes in Table 1. When possible, these bounds are 25% greater (lower) than the maximum (minimum) biological parameter values found in the literature. The mean, median, standard deviation, and percentiles (5th, 25th, 75th, 95th) of annual harvest yields resulting from these Monte Carlo simulations were calculated across each model grid cell. The relative importance of each Monte Carlo parameter value upon harvested biomass was evaluated using random forest analysis.

## Model Limitations

G-MACMODS and our scenarios are subject to a number of important limitations and caveats. First, neither of the implemented nutrient scenarios consider how seaweed farms affect the surrounding hydrodynamics, which can substantially affect nutrient uptake and yields[32] but are challenging to resolve in a global-scale model. Moreover, the nutrient data (from CESM simulations) do not resolve nutrient runoff in coastal areas[97], sources of nitrogen other than nitrate (e.g., ammonia or urea), nor consider other limiting macronutrients such as phosphate. These nutrient-related limitations may affect our harvest estimates in specific locations, and perhaps lead us to underestimate harvest in some nearshore areas. On the other hand, operating farms will not have the benefit of hindsight that our model uses to optimize seeding and harvest schedules, and the model assumptions are optimistic with regard to micronutrient fertilization and environment/strain optimization in cultivars. G-MACMODS would also benefit from a more refined expression of seaweed mortality that could account for episodic events (e.g. storms, diseases) and nonlinear grazing pressure, among other factors. Finally, we do not explicitly model the effects of climate change and projected changes in ocean conditions that can stress growing seaweeds, shift their geographical distribution, increase the frequency and severity of storms, decrease nutrient fluxes by enhanced stratification, and make diseases and epiphytes more prevalent[98,99]. The are important areas for future research. Although certainly not a proxy for the many effects of climate change, we note that interannual variability in environmental forcing 2003-2019 affects our harvest estimates less than the uncertainties related to biological parameters (Supplementary Fig. 10).

**Table 1.** Biological Parameters

| Parameter | Genus | Standard Values | Monte Carlo Bounds | References |
|---|---|---|---|---|
| $V_{max}$ | | | | |
| ($\mu$mol-N/(g-DW h)) | *Eucheuma* | 9.7 | [4.05, 16.3] | 100, 101 |
| Maximum uptake rate | | | | |
| | *Sargassum* | 17.9 | [1.86, 36.9] | 102, 103 |
| | *Porphyra* | 52.2 | [26.3, 90] | 104, 105, 106, 107 |
| | *Macrocystis* | 12.8 | [2.3, 38.1] | 108, 109, 110, 111, 112 |
| | *Saccharina* | 11.8 | [1.9, 30] | 113 , 29 |
| $K_m$ | | | | |
| ($\mu$M) | *Eucheuma* | 5.6 | [0.2, 13.8] | 100 |
| Half-saturation constant | | | | |
| | *Sargassum* | 3.0 | [1.1, 5.5] | 103 |
| | *Porphyra* | 5.2 | [1.5, 12.7] | |
| | *Macrocystis* | 10.1 | [3.2, 18.1] | 108, 109, 111 |
| | *Saccharina* | 2 | [1.1, 4.2] | 114, 113 |
| $\mu_{max}$ | | | | |
| (1/day) | *Eucheuma* | 0.2 | [0.1, 0.3] | 115, 116, 117 |
| Maximum growth rate | | | | |
| | *Sargassum* | 0.2 | [0.1, 0.3] | 118, 119 |
| | *Porphyra* | 0.2 | [0.1, 0.3] | 104, 120 |
| | *Macrocystis* | 0.2 | [0.1, 0.3] | 121, 122 |
| | *Saccharina* | 0.2 | [0.1, 0.3] | 123, 124, 125, 126 |
| $PAR_s$ | | | | |
| ($\mu$mol photon/(m$^2$ s)) | *Eucheuma* | 125.9 | [52.1, 550] | 127, 128, 129, 130, 131 |
| Saturating irradiance | | | | |
| | *Sargassum* | 303.9 | [112.5, 643.8] | 119, 132 |

**Table 1 – continued from previous page**

| Parameter | Genus | Standard Values | Monte Carlo Bounds | References |
|---|---|---|---|---|
| | *Porphyra* | 104 | [34.5, 233.8] | 133, 134 |
| | *Macrocystis* | 212.4 | [105.8, 350] | 135, 136 |
| | *Saccharina* | 76.3 | [11.3, 212.5] | 137, 138, 113 |
| $PAR_c$ ($\mu$mol photon/(m$^2$ s)) Compensating irradiance | *Eucheuma* | 13.5 | [3.8, 32.5] | 127, 128, 129, 130, 131 |
| | *Sargassum* | 26 | [3.8, 46.3] | 119, 132 |
| | *Porphyra* | 24.8 | [6.8, 54] | 133, 134 |
| | *Macrocystis* | 20.5 | [7.5, 43.1] | 135, 136 |
| | *Saccharina* | 15.5 | [5.7, 29.3] | 137, 113 |
| $Q_{min}$ (mg-N/g-DW) Minimum nitrogen cell quota | *Eucheuma* | 5.8 | [4.3, 7.2] | 139 |
| | *Sargassum* | 5.8 | [4.3, 7.2] | 139 |
| | *Porphyra* | 10.2 | [7.6, 12.7] | 139 |
| | *Macrocystis* | 10.2 | [7.6, 12.7] | 139 |
| | *Saccharina* | 10.2 | [7.6, 12.7] | 139 |
| $Q_{max}$ (mg-N/g-DW) Maximum nitrogen cell quota | *Eucheuma* | 44 | [33, 55] | 139 |
| | *Sargassum* | 44 | [33, 55] | 139 |
| | *Porphyra* | 54 | [40.5, 67.5] | 139 |
| | *Macrocystis* | 54 | [40.5, 67.5] | 139 |
| | *Saccharina* | 54 | [40.5, 67.5] | 139 |
| $C_D$ (unitless) Drag coefficient | *Eucheuma* | 0.5 | [0.01, 1] | |
| | *Sargassum* | 0.5 | [0.01, 1] | |
| | *Porphyra* | 0.5 | [0.01, 1] | |
| | *Macrocystis* | 0.5 | [0.01, 1] | 69 |
| | *Saccharina* | 0.5 | [0.01, 1] | 140 |
| B:SA (g-DW/m$^2$) Ratio of biomass to surface area | *Eucheuma* | 94.8 | [71.1, 118.5] | L. Roberson (personal comm.) |
| | *Sargassum* | 333 | [249.8, 416.3] | 29 |
| | *Porphyra* | 10 | [7.5, 12.5] | |
| | *Macrocystis* | 58 | [43.5, 72.5] | 108, 111, 110, 141 |
| | *Saccharina* | 58 | [43.5, 72.5] | |
| E (1/day) Exudation | *Eucheuma* | 0.05 | [0.001 0.1] | 36, 43, 51 |
| | *Sargassum* | 0.05 | [0.001 0.1] | 36, 43, 51 |
| | *Porphyra* | 0.05 | [0.001 0.1] | 36, 43, 51 |
| | *Macrocystis* | 0.05 | [0.001 0.1] | 36, 43, 51 |
| | *Saccharina* | 0.05 | [0.001 0.1] | 36, 43, 51 |
| d (1/day) Death rate | *Eucheuma* | 0.01 | [0.003 0.03] | 28, 29, 36, 43, 79 |
| | *Sargassum* | 0.01 | [0.003 0.03] | 28, 29, 36, 43, 79 |
| | *Porphyra* | 0.01 | [0.003 0.03] | 28, 29, 36, 43, 79 |
| | *Macrocystis* | 0.01 | [0.003 0.03] | 28, 29, 36, 43, 79 |
| | *Saccharina* | 0.01 | [0.003 0.03] | 28, 29, 36, 43, 79 |

**Table 2.** Temperature Parameters used in Equation 6

| Genus | $T_{opt}$ (°C) | $\beta_1$ | $\beta_2$ | References |
|---|---|---|---|---|
| *Eucheuma* | 22.5-27.5 | 0.09 | 0.09 | 142–144 |
| *Sargassum* | 22.5-27.5 | 0.09 | 0.09 | 145, 146 |
| *Porphyra* | 12-17 | 0.03 | 0.09 | 134, 147 |
| *Macrocystis* | 13-18 | 0.04 | 0.05 | 148, 149 |
| *Saccharina* | 10-15 | 0.03 | 0.1 | 124, 126, 138 |

## References


1. DeAngelo, J. *et al.* Energy systems in scenarios at net-zero $CO_2$ emissions. *Nat. Commun.* **12**, 1–10, DOI: 10.1038/s41467-021-26356-y (2021).
2. IPCC. Summary for Policymakers. *Clim. Chang. 2021: The Phys. Sci. Basis. Contribution Work. Group I to Sixth Assess. Rep. Intergov. Panel on Clim. Chang.* (2021).
3. DeVries, T., Holzer, M. & Primeau, F. Recent increase in oceanic carbon uptake driven by weaker upper-ocean overturning. *Nature* **542**, 215–218, DOI: 10.1038/nature21068 (2017).
4. Friedlingstein, P. *et al.* Global Carbon Budget 2021. *Earth Syst. Sci. Data Discuss.* 1–191, DOI: 10.5194/essd-2021-386 (2021).
5. National Academies of Sciences, Engineering, and Medicine. A Research Strategy for Ocean-Based Carbon Dioxide Removal and Sequestration. DOI: 10.17226/26278 (2021).
6. Froehlich, H. E., Afflerbach, J. C., Frazier, M. & Halpern, B. S. Blue growth potential to mitigate climate change through seaweed offsetting. *Curr. Biol.* **29**, 3087–3093, DOI: 10.1016/j.cub.2019.07.041 (2019).
7. Duarte, C. M., Bruhn, A. & Krause-Jensen, D. A seaweed aquaculture imperative to meet global sustainability targets. *Nat. Sustain.* 1–9, DOI: 10.1038/s41893-021-00773-9 (2021).
8. Milledge, J. J., Smith, B., Dyer, P. W. & Harvey, P. Macroalgae-derived biofuel: a review of methods of energy extraction from seaweed biomass. *Energies* **7**, 7194–7222, DOI: 10.3390/en7117194 (2014).
9. Michalak, I. Experimental processing of seaweeds for biofuels. *Wiley Interdiscip. Rev. Energy Environ.* **7**, e288, DOI: 10.1002/wene.288 (2018).
10. Ravanal, M. C. *et al.* Production of bioethanol from brown algae. In *Advances in Feedstock Conversion Technologies for Alternative Fuels and Bioproducts*, 69–88 (Elsevier, 2019).
11. Vijn, S. *et al.* Key considerations for the use of seaweed to reduce enteric methane emissions from cattle. *Front. Vet. Sci.* **7**, 1135, DOI: 10.3389/fvets.2020.597430 (2020).
12. Roque, B. M. *et al.* Red seaweed (Asparagopsis taxiformis) supplementation reduces enteric methane by over 80 percent in beef steers. *Plos one* **16**, e0247820, DOI: 10.1371/journal.pone.0247820 (2021).
13. He, P. *et al.* Bioremediation efficiency in the removal of dissolved inorganic nutrients by the red seaweed, *Porphyra yezoensis*, cultivated in the open sea. *Water Res.* **42**, 1281–1289, DOI: 10.1016/j.watres.2007.09.023 (2008).
14. Huo, Y. Z. *et al.* Bioremediation efficiencies of *Gracilaria verrucosa* cultivated in an enclosed sea area of Hangzhou Bay, China. *J. Appl. Phycol.* **23**, 173–182, DOI: 10.1007/s10811-010-9584-9 (2011).
15. Xiao, X. *et al.* Nutrient removal from Chinese coastal waters by large-scale seaweed aquaculture. *Sci. Reports* **7**, 1–6, DOI: 10.1038/srep46613 (2017).
16. Jiang, Z. *et al.* Kelp cultivation effectively improves water quality and regulates phytoplankton community in a turbid, highly eutrophic bay. *Sci. Total. Environ.* **707**, 135561, DOI: 10.1016/j.scitotenv.2019.135561 (2020).
17. Bhuyan, M., Islam, M., Sharif, A. S. M., Hoq, M. *et al.* Seaweed: A Powerful Tool for Climate Change Mitigation That Provides Various Ecological Services. *Bangladesh II: Clim. Chang. Impacts, Mitig. Adapt. Dev. Ctries.* 159–192 (2021).
18. FAO. *The state of world fisheries and aquaculture 2020: Sustainability in action* (Food and Agriculture Organization of the United Nations, 2020).
19. Bak, U. G., Mols-Mortensen, A. & Gregersen, O. Production method and cost of commercial-scale offshore cultivation of kelp in the Faroe Islands using multiple partial harvesting. *Algal research* **33**, 36–47, DOI: 10.1016/j.algal.2018.05.001 (2018).
20. Buck, B. H. *et al.* State of the art and challenges for offshore integrated multi-trophic aquaculture (IMTA). *Front. Mar. Sci.* **5**, 165, DOI: 10.3389/fmars.2018.00165 (2018).
21. Azevedo, I. C., Duarte, P. M., Marinho, G. S., Neumann, F. & Sousa-Pinto, I. Growth of *Saccharina latissima* (*Laminariales*, *Phaeophyceae*) cultivated offshore under exposed conditions. *Phycologia* **58**, 504–515, DOI: 10.1080/00318884.2019.1625610 (2019).
22. Navarrete, I. A. *et al.* Effects of depth-cycling on nutrient uptake and biomass production in the giant kelp *Macrocystis pyrifera*. *Renew. Sustain. Energy Rev.* **141**, 110747, DOI: 10.1016/j.rser.2021.110747 (2021).

**23.** Solvang, T., Bale, E. S., Broch, O. J., Handå, A. & Alver, M. O. Automation Concepts for Industrial-Scale Production of Seaweed. *Front. Mar. Sci.* DOI: 10.3389/fmars.2021.613093 (2021).

**24.** Chung, I. K., Beardall, J., Mehta, S., Sahoo, D. & Stojkovic, S. Using marine macroalgae for carbon sequestration: a critical appraisal. *J. applied phycology* **23**, 877–886, DOI: 10.1007/s10811-010-9604-9 (2011).

**25.** Krause-Jensen, D. & Duarte, C. M. Substantial role of macroalgae in marine carbon sequestration. *Nat. Geosci.* **9**, 737–742, DOI: 10.1038/ngeo2790 (2016).

**26.** Solidoro, C., Pecenik, G., Pastres, R., Franco, D. & Dejak, C. Modelling macroalgae (*Ulva rigida*) in the Venice lagoon: Model structure identification and first parameters estimation. *Ecol. Model.* **94**, 191–206, DOI: 10.1016/S0304-3800(96)00025-7 (1997).

**27.** Broch, O. J. & Slagstad, D. Modelling seasonal growth and composition of the kelp *Saccharina latissima*. *J. applied phycology* **24**, 759–776, DOI: 10.1007/s10811-011-9695-y (2012).

**28.** Hadley, S., Wild-Allen, K., Johnson, C. & Macleod, C. Modeling macroalgae growth and nutrient dynamics for integrated multi-trophic aquaculture. *J. Appl. Phycol.* **27**, 901–916, DOI: 10.1007/s10811-014-0370-y (2015).

**29.** Zhang, J., Wu, W., Ren, J. S. & Lin, F. A model for the growth of mariculture kelp *Saccharina japonica* in Sanggou Bay, China. *Aquac. Environ. Interactions* **8**, 273–283, DOI: 10.3354/aei00171 (2016).

**30.** Molen, J. v. d. *et al.* Modelling potential production of macroalgae farms in UK and Dutch coastal waters. *Biogeosciences* **15**, 1123–1147, DOI: 10.5194/bg-15-1123-2018 (2018).

**31.** Wu, J., Keller, D. P. & Oschlies, A. Carbon Dioxide Removal via Macroalgae Open-ocean Mariculture and Sinking: An Earth System Modeling Study. *Earth Syst. Dynam.* **preprint**, DOI: 10.5194/esd-2021-104 (2022).

**32.** Frieder, C. *et al.* A Macroalgal Cultivation Modeling System (MACMODS): Evaluating the Role of Physical-Biological Coupling on Nutrients and Farm Yield. *Front. Mar. Sci.* **Accepted article**, DOI: 10.3389/fmars.2021.752951 (2022).

**33.** Brush, M. J. & Nixon, S. W. Modeling the role of macroalgae in a shallow sub-estuary of Narragansett Bay, RI (USA). *Ecol. Model.* **221**, 1065–1079, DOI: 10.1016/j.ecolmodel.2009.11.002 (2010).

**34.** Behrenfeld, M. J. & Falkowski, P. G. Photosynthetic rates derived from satellite-based chlorophyll concentration. *Limnol. oceanography* **42**, 1–20, DOI: 10.4319/lo.1997.42.1.0001 (1997).

**35.** Siegel, D. *et al.* Global assessment of ocean carbon export by combining satellite observations and food-web models. *Glob. Biogeochem. Cycles* **28**, 181–196, DOI: 10.1002/2013GB004743 (2014).

**36.** Rassweiler, A., Reed, D. C., Harrer, S. L. & Nelson, J. C. Improved estimates of net primary production, growth, and standing crop of *Macrocystis pyrifera* in Southern California, DOI: 10.1002/ecy.2440 (2018).

**37.** Zhu, G., Ebbing, A., Bouma, T. J. & Timmermans, K. R. Morphological and physiological plasticity of *Saccharina latissima* (*Phaeophyceae*) in response to different hydrodynamic conditions and nutrient availability. *J. Appl. Phycol.* 1–13, DOI: 10.1007/s10811-021-02428-w (2021).

**38.** Andersson, M., Schubert, H., Pedersén, M. & Snoeijs, P. Different patterns of carotenoid composition and photosynthesis acclimation in two tropical red algae. *Mar. Biol.* **149**, 653–665, DOI: 10.1007/s00227-005-0174-3 (2006).

**39.** Freile-Pelegrín, Y. & Robledo, D. Carrageenan of *Eucheuma isiforme* (Solieriaceae, Rhodophyta) from Yucatán, Mexico. II. Seasonal variations in carrageenan and biochemical characteristics. DOI: 10.1515/BOT.2006.009 (2006).

**40.** Roberts, D. A., Paul, N. A., Dworjanyn, S. A., Bird, M. I. & de Nys, R. Biochar from commercially cultivated seaweed for soil amelioration. *Sci. reports* **5**, 1–6, DOI: 10.1038/srep09665 (2015).

**41.** Martin, J. H. *et al.* Testing the iron hypothesis in ecosystems of the equatorial Pacific Ocean. *Nature* **371**, 123–129, DOI: 10.1038/371123a0 (1994).

**42.** Moore, J. K., Doney, S. C., Glover, D. M. & Fung, I. Y. Iron cycling and nutrient-limitation patterns in surface waters of the World Ocean. *Deep. Sea Res. Part II: Top. Stud. Oceanogr.* **49**, 463–507, DOI: 10.1016/S0967-0645(01)00109-6 (2001).

**43.** Wool, T. A. WASP8 Macro Algae-Model Theory and User's Guide. .

**44.** Trancoso, A. *et al.* Modelling macroalgae using a 3D hydrodynamic-ecological model in a shallow, temperate estuary. *Ecol. Model.* **187**, 232–246, DOI: 10.1016/j.ecolmodel.2005.01.054 (2005).

**45.** Hwang, E. K., Yotsukura, N., Pang, S. J., Su, L. & Shan, T. F. Seaweed breeding programs and progress in eastern Asian countries. *Phycologia* **58**, 484–495, DOI: 10.1080/00318884.2019.1639436 (2019).

**46.** USGS. Map of Croplands in the United States. https://www.usgs.gov/media/images/map-croplands-united-states#:~:text=The%20United%20States%20has%20166,180%20million%20hectares%20of%20croplands. Accessed on 4 February 2022.

**47.** Bach, L. T. *et al.* Testing the climate intervention potential of ocean afforestation using the Great Atlantic *Sargassum* Belt. *Nat. communications* **12**, 1–10, DOI: 10.1038/s41467-021-22837-2 (2021).

**48.** Ren, J. S., Stenton-Dozey, J., Plew, D. R., Fang, J. & Gall, M. An ecosystem model for optimising production in integrated multitrophic aquaculture systems. *Ecol. Model.* **246**, 34–46, DOI: 10.1016/j.ecolmodel.2012.07.020 (2012).

**49.** Duarte, P. & Ferreira, J. A model for the simulation of macroalgal population dynamics and productivity. *Ecol. modelling* **98**, 199–214, DOI: 10.1016/S0304-3800(96)01915-1 (1997).

**50.** Kambey, C. S. *et al.* Seaweed aquaculture: a preliminary assessment of biosecurity measures for controlling the ice-ice syndrome and pest outbreaks of a *Kappaphycus* farm. *J. Appl. Phycol.* **33**, 3179–3197, DOI: 10.1007/s10811-021-02530-z (2021).

**51.** Chen, S. *et al.* Release of dissolved and particulate organic matter by marine macroalgae and its biogeochemical implications. *Algal Res.* **52**, 102096, DOI: 10.1016/j.algal.2020.102096 (2020).

**52.** Haas, A. F. *et al.* Organic matter release by coral reef associated benthic algae in the Northern Red Sea. *J. Exp. Mar. Biol. Ecol.* **389**, 53–60, DOI: 10.1016/j.jembe.2010.03.018 (2010).

**53.** Reed, D. C. *et al.* Patterns and controls of reef-scale production of dissolved organic carbon by giant kelp *Macrocystis pyrifera*. *Limnol. Oceanogr.* **60**, 1996–2008, DOI: 10.1002/lno.10154 (2015).

**54.** Paine, E. R., Schmid, M., Boyd, P. W., Diaz-Pulido, G. & Hurd, C. L. Rate and fate of dissolved organic carbon release by seaweeds: A missing link in the coastal ocean carbon cycle. *J. Phycol.* **57**, 1375–1391, DOI: 10.1111/jpy.13198 (2021).

**55.** Gordillo, F. J., Niell, F. X. & Figueroa, F. L. Non-photosynthetic enhancement of growth by high $CO_2$ level in the nitrophilic seaweed *Ulva rigida* C. Agardh (Chlorophyta). *Planta* **213**, 64–70, DOI: 10.1007/s004250000468 (2001).

**56.** Livanou, E., Lagaria, A., Psarra, S. & Lika, K. A DEB-based approach of modeling dissolved organic matter release by phytoplankton. *J. Sea Res.* **143**, 140–151, DOI: 10.1016/j.seares.2018.07.016 (2019).

**57.** Wyatt, K. H., Tellez, E., Woodke, R. L., Bidner, R. J. & Davison, I. R. Effects of nutrient limitation on the release and use of dissolved organic carbon from benthic algae in Lake Michigan. *Freshw. Sci.* **33**, 557–567, DOI: 10.1086/675453 (2014).

**58.** Koivikko, R., Loponen, J., Honkanen, T. & Jormalainen, V. Contents of soluble, cell-wall-bound and exuded phlorotannins in the brown alga *Fucus vesiculosus*, with implications on their ecological functions. *J. chemical ecology* **31**, 195–212, DOI: 10.1007/s10886-005-0984-2 (2005).

**59.** Smith, C. R., De Leo, F. C., Bernardino, A. F., Sweetman, A. K. & Arbizu, P. M. Abyssal food limitation, ecosystem structure and climate change. *Trends Ecol. & Evol.* **23**, 518–528, DOI: 10.1016/j.tree.2008.05.002 (2008).

**60.** Smith, C. R. *et al.* Latitudinal variations in benthic processes in the abyssal equatorial Pacific: control by biogenic particle flux. *Deep. Sea Res. Part II: Top. Stud. Oceanogr.* **44**, 2295–2317, DOI: 10.1016/S0967-0645(97)00022-2 (1997).

**61.** Nomaki, H. *et al.* In situ experimental evidences for responses of abyssal benthic biota to shifts in phytodetritus compositions linked to global climate change. *Glob. Chang. Biol.* **27**, 6139–6155, DOI: 10.1111/gcb.15882 (2021).

**62.** Jarvis, B. M. *et al.* Modeling spatiotemporal patterns of ecosystem metabolism and organic carbon dynamics affecting hypoxia on the Louisiana Continental Shelf. *J. Geophys. Res. Ocean.* **125**, e2019JC015630, DOI: 10.1029/2019JC015630 (2020).

**63.** Yu, L., Fennel, K., Laurent, A., Murrell, M. C. & Lehrter, J. C. Numerical analysis of the primary processes controlling oxygen dynamics on the Louisiana shelf. *Biogeosciences* **12**, 2063–2076, DOI: 10.5194/bg-12-2063-2015 (2015).

**64.** Droop, M. R. Some thoughts on nutrient limitation in algae. *J. phycology* **9**, 264–272, DOI: 10.1111/j.1529-8817.1973.tb04092.x (1973).

**65.** Pessarrodona, A., Moore, P. J., Sayer, M. D. & Smale, D. A. Carbon assimilation and transfer through kelp forests in the NE Atlantic is diminished under a warmer ocean climate. *Glob. Chang. Biol.* **24**, 4386–4398, DOI: 10.1111/gcb.14303 (2018).

**66.** Visch, W., Nylund, G. M. & Pavia, H. Growth and biofouling in kelp aquaculture (*Saccharina latissima*): the effect of location and wave exposure. *J. Appl. Phycol.* **32**, 3199–3209, DOI: 10.1007/s10811-020-02201-5 (2020).

**67.** Fram, J. P. *et al.* Physical pathways and utilization of nitrate supply to the giant kelp, *Macrocystis pyrifera*. *Limnol. Oceanogr.* **53**, 1589–1603, DOI: 10.4319/lo.2008.53.4.1589 (2008).

**68.** Sanford, L. P. & Crawford, S. M. Mass transfer versus kinetic control of uptake across solid-water boundaries. *Limnol. Oceanogr.* **45**, 1180–1186, DOI: 10.4319/lo.2000.45.5.1180 (2000).

**69.** Stevens, C. L. & Hurd, C. L. Boundary-layers around bladed aquatic macrophytes. *Hydrobiologia* **346**, 119–128, DOI: 10.1023/A:1002914015683 (1997).

**70.** Yuan-Hui, L. & Gregory, S. Diffusion of ions in sea water and in deep-sea sediments. *Geochimica et cosmochimica acta* **38**, 703–714, DOI: 10.1016/0016-7037(74)90145-8 (1974).

**71.** Dade, W. B. Near-bed turbulence and hydrodynamic control of diffusional mass transfer at the sea floor. *Limnol. Oceanogr.* **38**, 52–69, DOI: 10.4319/lo.1993.38.1.0052 (1993).

**72.** Stevens, C. L., Hurd, C. L. & Isachsen, P. E. Modelling of diffusion boundary-layers in subtidal macroalgal canopies: The response to waves and currents. *Aquatic sciences* **65**, 81–91, DOI: 10.1007/s000270300007 (2003).

**73.** Huang, I., Rominger, J. & Nepf, H. The motion of kelp blades and the surface renewal model. *Limnol. oceanography* **56**, 1453–1462, DOI: 10.4319/lo.2011.56.4.1453 (2011).

**74.** Xiao, X. *et al.* Resource (light and nitrogen) and density-dependence of seaweed growth. *Front. Mar. Sci.* **6**, 618, DOI: 10.3389/fmars.2019.00618 (2019).

**75.** Cerco, C. & Cole, T. M. User's guide to the CE-QUAL-ICM three-dimensional eutrophication model: release version 1.0. (1995).

**76.** Di Toro, D. M., O'CONNOR, D. J. & Thomann, R. V. A dynamic model of the phytoplankton population in the Sacramento—San Joaquin Delta. DOI: 10.1021/ba-1971-0106.ch005 (1971).

**77.** Long, M. C. *et al.* Simulations with the Marine Biogeochemistry Library (MARBL). *J. Adv. Model. Earth Syst.* **13**, DOI: 10.1029/2021MS002647 (2021).

**78.** MARBL Developers. *MARBL Documentation*. NCAR.

**79.** Duarte, P. & Ferreira, J. A methodology for parameter estimation in seaweed productivity modelling. In *Fourteenth International Seaweed Symposium*, 183–189, DOI: 10.1007/978-94-011-1998-6_22 (Springer, 1993).

**80.** Wallcraft, A., Metzger, E. & Carroll, S. Software design description for the hybrid coordinate ocean model (HYCOM), Version 2.2. Tech. Rep., NAVAL RESEARCH LAB STENNIS SPACE CENTER MS OCEANOGRAPHY DIV (2009).

**81.** Cummings, J. A. Operational multivariate ocean data assimilation. *Q. J. Royal Meteorol. Soc. A journal atmospheric sciences, applied meteorology physical oceanography* **131**, 3583–3604, DOI: 10.1256/qj.05.105 (2005).

**82.** Hersbach, H. *et al.* The ERA5 global reanalysis. *Q. J. Royal Meteorol. Soc.* **146**, 1999–2049, DOI: 10.1002/qj.3803 (2020).

**83.** C3S. ERA5: Fifth generation of ECMWF atmospheric reanalyses of the global climate. https://cds.climate.copernicus.eu/cdsapp#!/dataset/reanalysis-era5-single-levels?tab=form (2017). Accessed using Copernicus Climate Change Service Climate Data Store (CDS).

**84.** Hurrell, J. W. *et al.* The Community Earth System Model: a framework for collaborative research. *Bull. Am. Meteorol. Soc.* **94**, 1339–1360, DOI: 10.1175/BAMS-D-12-00121.1 (2013).

**85.** Harrison, C. S., Long, M. C., Lovenduski, N. S. & Moore, J. K. Mesoscale effects on carbon export: A global perspective. *Glob. Biogeochem. Cycles* **32**, 680–703, DOI: 10.1002/2017GB005751 (2018).

**86.** Ferdouse, F., Holdt, S. L., Smith, R., Murúa, P. & Yang, Z. The global status of seaweed production, trade and utilization. *Globefish Res. Programme* **124**, I (2018).

**87.** Wakibia, J., Ochiewo, J. & Bolton, J. J. Economic analysis of eucheumoid algae farming in Kenya. *West. Indian Ocean. J. Mar. Sci.* **10**, 13–24 (2011).

**88.** Periyasamy, C., Rao, P. S. & Anantharaman, P. Harvest optimization to assess sustainable growth and carrageenan yield of cultivated *Kappaphycus alvarezii* (Doty) Doty in Indian waters. *J. Appl. Phycol.* **31**, 587–597, DOI: 10.1007/s10811-018-1562-7 (2019).

**89.** Kumar, K. S., Ganesan, K., Rao, P. S. & Thakur, M. Seasonal studies on field cultivation of *Kappaphycus alvarezii* (Doty) Doty on the northwest coast of India. *J. applied phycology* **28**, 1193–1205, DOI: 10.1007/s10811-015-0629-y (2016).

**90.** Wijayanto, D., Bambang, A. N., Nugroho, R. A. & Kurohman, F. The impact of planting distance on productivity and profit of *Eucheuma cottonii* seaweed cultivation in Karimunjawa Islands, Indonesia. *Aquac. Aquarium, Conserv. & Legislation* **13**, 2170–2179 (2020).

**91.** Neish, I. C. Social and economic dimensions of carrageenan seaweed farming in Indonesia. *Soc. Econ. Dimensions Carrageenan Seaweed Farming. Fish. Aquac. Tech. Pap. No. 580* (2013).

**92.** Hurtado, A. Q. Social and economic dimensions of carrageenan seaweed farming in the Philippines. *Soc. Econ. Dimensions Carrageenan Seaweed Farming. Fish. Aquac. Tech. Pap. No. 580* (2013).

**93.** Wang, X. *et al.* Economically important red algae resources along the Chinese coast: History, status, and prospects for their utilization. *Algal Res.* **46**, 101817, DOI: 10.1016/j.algal.2020.101817 (2020).

**94.** Marinho, G. S., Holdt, S. L., Birkeland, M. J. & Angelidaki, I. Commercial cultivation and bioremediation potential of sugar kelp, *Saccharina latissima*, in Danish waters. *J. applied phycology* **27**, 1963–1973, DOI: 10.1007/s10811-014-0519-8 (2015).

**95.** Camus, C., Infante, J. & Buschmann, A. H. Overview of 3 year precommercial seafarming of *Macrocystis pyrifera* along the Chilean coast. *Rev. Aquac.* **10**, 543–559, DOI: 10.1111/raq.12185 (2018).

**96.** Msuya, F. E. *et al.* A comparative economic analysis of two seaweed farming methods in Tanzania. *The Sustain. Coast. Communities Ecosyst. Program. Coast. Resour. Center, Univ. Rhode Island West. Indian Ocean. Mar. Sci. Assoc.* (2007).

**97.** McPhee-Shaw, E. E. *et al.* Mechanisms for nutrient delivery to the inner shelf: Observations from the Santa Barbara Channel. *Limnol. Oceanogr.* **52**, 1748–1766, DOI: 10.4319/lo.2007.52.5.1748 (2007).

**98.** Largo, D. B., Fukami, K., Nishijima, T. & Ohno, M. Laboratory-induced development of the ice-ice disease of the farmed red algae *Kappaphycus alvarezii* and *Eucheuma denticulatum* (Solieriaceae, Gigartinales, Rhodophyta). *J. Appl. Phycol.* **7**, 539–543, DOI: 10.1007/BF00003940 (1995).

**99.** Largo, D. B., Msuya, F. E. & Menezes, A. Understanding diseases and control in seaweed farming in Zanzibar. *FAO Fish. Aquac. Tech. Pap.* 0_1–49 (2020).

**100.** Cabello-Pasini, A., Zertuche-González, J. A. & Pacheco-Ruíz, I. Photosynthesis, growth and nitrogen uptake of competing marine macrophytes in the Gulf of California. DOI: 10.1515/BOT.2003.052 (2003).

**101.** Nishihara, G. N. & Terada, R. Spatial variations in nutrient supply to the red algae *Eucheuma serra* (J. Agardh) J. Agardh. *Phycol. research* **58**, 29–34, DOI: 10.1111/j.1440-1835.2009.00555.x (2010).

**102.** Jouanno, J. *et al.* A NEMO-based model of *Sargassum* distribution in the Tropical Atlantic: description of the model and sensitivity analysis (NEMO-Sarg1. 0). *Geosci. Model. Dev. Discuss.* 1–30, DOI: 10.5194/gmd-2020-383 (2020).

**103.** Ramalakshmi, Y. & Chauhan, D. Nitrate and ammonium uptake by alga *Sargassum swartzii* (Turn.) C. Ag.(Phaeophyta). (1990).

**104.** Carmona, R., Kraemer, G. & Yarish, C. Exploring Northeast American and Asian species of *Porphyra* for use in an integrated finfish–algal aquaculture system. *Aquaculture* **252**, 54–65, DOI: 10.1016/j.aquaculture.2005.11.049 (2006).

**105.** Kraemer, G. P. *et al.* Evaluation of the bioremediatory potential of several species of the red alga *Porphyra* using short-term measurements of nitrogen uptake as a rapid bioassay. *J. Appl. Phycol.* **16**, 489–497, DOI: 10.1007/s10811-004-5511-2 (2004).

**106.** Niwa, K. & Harada, K. Physiological responses to nitrogen deficiency and resupply in different blade portions of *Pyropia yezoensi*s f. narawaensis (Bangiales, Rhodophyta). *J. experimental marine biology ecology* **439**, 113–118, DOI: 10.1016/j.jembe.2012.10.017 (2013).

**107.** Pedersen, A., Kraemer, G. & Yarish, C. The effects of temperature and nutrient concentrations on nitrate and phosphate uptake in different species of *Porphyra* from Long Island Sound (USA). *J. Exp. Mar. Biol. Ecol.* **312**, 235–252, DOI: 10.1016/j.jembe.2004.05.021 (2004).

**108.** Gerard, V. In situ water motion and nutrient uptake by the giant kelp *Macrocystis pyrifera*. *Mar. biology* **69**, 51–54, DOI: 10.1007/BF00396960 (1982).

**109.** Gerard, V. A. In situ rates of nitrate uptake by giant kelp, *Macrocystis pyrifera* (L.) C. Agardh: tissue differences, environmental effects, and predictions of nitrogen-limited growth. *J. Exp. Mar. Biol. Ecol.* **62**, 211–224, DOI: 10.1016/0022-0981(82)90202-7 (1982).

**110.** Kopczak, C. D. Variability of nitrate uptake capacity in *Macrocystis Pyrifera* (Laminariales, Phaeophyta) with nitrate and light availability. *J. phycology* **30**, 573–580, DOI: 10.1111/j.0022-3646.1994.00573.x (1994).

**111.** Haines, K. C. & Wheeler, P. A. Ammoniun and nitrate uptake by the marine macrophytes *Hypnea musvuformis* (Rhodophyta) and *Macrocystis pyrifera* (phaeophyta) 1, 2. *J. Phycol.* **14**, 319–324, DOI: 10.1111/j.1529-8817.1978.tb00305.x (1978).

**112.** Sánchez-Barredo, M. *et al.* Effects of Heat Waves and Light Deprivation on Giant Kelp Juveniles (*Macrocystis pyrifera*, Laminariales, Phaeophyceae). *J. phycology* **56**, 880–894, DOI: 10.1111/jpy.13000 (2020).

**113.** Ozaki, A., Mizuta, H. & Yamamoto, H. Physiological differences between the nutrient uptakes of Kjellmaniella crassifolia and *Laminaria japonica* (*Phaeophycea*e). *Fish. science* **67**, 415–419, DOI: 10.1046/j.1444-2906.2001.00277.x (2001).

**114.** Chapman, A., Markham, J. & Lüning, K. Effects of nitrate concentration on the growth and physiology of *Laminaria saccharina* (Phaeophyta) in culture 1, 2. *J. phycology* **14**, 195–198, DOI: 10.1111/j.1529-8817.1978.tb02448.x (1978).

**115.** Msuya, F. E. & Salum, D. Effect of the presence of seagrass and nutrients on growth rates of farmed *Kappaphycus alvarezii* and *Eucheuma denticulatum* (Rhodophyta). *West. Indian Ocean. J. Mar. Sci.* **10**, 129–135 (2011).

**116.** Rosas, E. D. V. M., Cabrera, J. A. R., León, R. E. R. & Rodríguez, J. L. N. Evaluación del crecimiento de *Eucheuma isiforme* (Rhodophyta, Gigartinales) en sistemas de cultivo suspendidos en la isla de Cubagua, Venezuela (sureste del Mar Caribe). *AquaTechnica: Revista Iberoamericana de Acuicultura.* **2**, 86–98 (2020).

**117.** Wakibia, J., Bolton, J., Keats, D. & Raitt, L. Factors influencing the growth rates of three commercial eucheumoids at coastal sites in southern Kenya. *J. Appl. Phycol.* **18**, 565–573, DOI: 10.1007/s10811-006-9058-2 (2006).

**118.** Choi, H. G. *et al.* Physiological differences in the growth of *Sargassum horneri*between the germling and adult stages. In *Nineteenth International Seaweed Symposium*, 279–285, DOI: 10.1007/978-1-4020-9619-8_35 (Springer, 2007).

**119.** Hanisak, M. D. & Samuel, M. A. Growth rates in culture of several species of *Sargassum* from Florida, USA. In *Twelfth International Seaweed Symposium*, 399–404, DOI: 10.1007/978-94-009-4057-4_59 (Springer, 1987).

**120.** Gao, G., Gao, Q., Bao, M., Xu, J. & Li, X. Nitrogen availability modulates the effects of ocean acidification on biomass yield and food quality of a marine crop *Pyropia yezoensi*s. *Food chemistry* **271**, 623–629, DOI: 10.1016/j.foodchem.2018.07.090 (2019).

**121.** Kopczak, C. D. The effects of nitrate limitation on the growth and physiology of the giant kelp, *Macrocystis pyrifera* (Phaeophyta). (1994).

**122.** De Nys, R., Jameson, P., Chin, N., Brown, M. & Sanderson, K. The cytokinins as endogenous growth regulators in *Macrocystis pyrifera* (L.) C. Ag.(*Phaeophycea*e). *Bot. marina* **33**, 467–476 (1990).

**123.** Azevedo, I. C., Marinho, G. S., Silva, D. M. & Sousa-Pinto, I. Pilot scale land-based cultivation of *Saccharina latissima* Linnaeus at southern European climate conditions: growth and nutrient uptake at high temperatures. *Aquaculture* **459**, 166–172, DOI: 10.1016/j.aquaculture.2016.03.038 (2016).

**124.** Bolton, J. & Lüning, K. Optimal growth and maximal survival temperatures of Atlantic Laminaria species (Phaeophyta) in culture. *Mar. Biol.* **66**, 89–94, DOI: 10.1007/BF00397259 (1982).

**125.** Freitas, J. R., Morrondo, J. M. S. & Ugarte, J. C. *Saccharina latissima* (Laminariales, Ochrophyta) farming in an industrial IMTA system in Galicia (Spain). *J. applied phycology* **28**, 377–385, DOI: 10.1007/s10811-015-0526-4 (2016).

**126.** Gao, X., Endo, H., Nagaki, M. & Agatsuma, Y. Interactive effects of nutrient availability and temperature on growth and survival of different size classes of *Saccharina japonica* (Laminariales, Phaeophyceae). *Phycologia* **56**, 253–260, DOI: 10.2216/16-91.1 (2017).

**127.** Borlongan, I. A., Gerung, G. S., Kawaguchi, S., Nishihara, G. N. & Terada, R. Thermal and PAR effects on the photosynthesis of *Eucheuma denticulatum* and *Kappaphycus striatus* (so-called Sacol strain) cultivated in shallow bottom of Bali, Indonesia. *J. Appl. Phycol.* **29**, 395–404, DOI: 10.1007/s10811-016-0956-7 (2017).

**128.** Borlongan, I. A., Nishihara, G. N., Shimada, S. & Terada, R. Effects of temperature and PAR on the photosynthesis of *Kappaphycus* sp.(Solieriaceae, Rhodophyta) from Okinawa, Japan, at the northern limit of native *Kappaphycus* distribution in the western Pacific. *Phycologia* **56**, 444–453, DOI: 10.2216/16-140.1 (2017).

**129.** Dangan-Galon, F. D., Dumilag, R. V. & Ganzon-Fortes, E. Photosynthesis-irradiance curves of four marine macroalgae from Bolinao, Pangasinan and Calatagan, Batangas, Philippines. *Sch. J. Sci. Res. Essay (SJSRE)* **2**, 134–138 (2013).

**130.** Dawes, C. Irradiance acclimation of the cultured Philippine seaweeds, *Kappaphycus alvarezii* and *Eucheuma denticulatum*. DOI: 10.1515/botm.1992.35.3.189 (1992).

**131.** Nishihara, G. N., Noro, T., Terada, R. *et al.* In vitro growth and photosynthesis of three edible seaweeds, *Betaphycus gelatinus*, *Eucheuma serra* and *Meristotheca papulosa* (Solieriaceae, Rhodophyta). *Aquac. Sci.* **59**, 563–571 (2011).

**132.** Kokubu, S. *et al.* The effect of irradiance and temperature on the photosynthesis of a native alga *Sargassum* fusiforme (Fucales) from Kagoshima, Japan. *Phycologia* **54**, 235–247, DOI: 10.2216/15-007.1 (2015).

**133.** Watanabe, Y., Nishihara, G. N., Tokunaga, S. & Terada, R. Effect of irradiance and temperature on the photosynthesis of a cultivated red alga, *Pyropia tenera* (*Porphyra tenera*), at the southern limit of distribution in J apan. *Phycol. research* **62**, 187–196, DOI: 10.1111/pre.12053 (2014).

**134.** Watanabe, Y. *et al.* Photosynthetic responses of *Pyropia yezoensis* f. narawaensis (Bangiales, Rhodophyta) to a thermal and PAR gradient vary with the life-history stage. *Phycologia* **55**, 665–672, DOI: 10.2216/16-25.1 (2016).

**135.** Gerard, V. Photosynthetic characteristics of giant kelp (*Macrocystis pyrifera*) determined in situ. *Mar. Biol.* **90**, 473–482 (1986).

**136.** Umanzor, S., Ramírez-García, M. M., Sandoval-Gil, J. M., Zertuche-González, J. A. & Yarish, C. Photoacclimation and Photoprotection of Juvenile Sporophytes of *Macrocystis pyrifera* (Laminariales, *Phaeophyceae*) Under High-light Conditions During Short-term Shallow-water Cultivation1. *J. phycology* **56**, 380–392, DOI: 10.1111/jpy.12951 (2020).

**137.** Borum, J., Pedersen, M., Krause-Jensen, D., Christensen, P. & Nielsen, K. Biomass, photosynthesis and growth of *Laminaria saccharina* in a high-arctic fjord, NE Greenland. *Mar. Biol.* **141**, 11–19, DOI: 10.1007/s00227-002-0806-9 (2002).

**138.** Fortes, M. & Lüning, K. Growth rates of North Sea macroalgae in relation to temperature, irradiance and photoperiod. *Helgoländer Meeresuntersuchungen* **34**, 15–29, DOI: 10.1007/BF01983538 (1980).

**139.** Angell, A. R., Mata, L., de Nys, R. & Paul, N. A. The protein content of seaweeds: a universal nitrogen-to-protein conversion factor of five. *J. Appl. Phycol.* **28**, 511–524, DOI: 10.1007/s10811-015-0650-1 (2016).

**140.** Vettori, D. & Nikora, V. Flow-seaweed interactions of *Saccharina latissima* at a blade scale: turbulence, drag force, and blade dynamics. *Aquatic Sci.* **81**, 1–16, DOI: 10.1007/s00027-019-0656-x (2019).

**141.** Wheeler, W. & Druehl, L. Seasonal growth and productivity of *Macrocystis integrifolia* in British Columbia, Canada. *Mar. Biol.* **90**, 181–186, DOI: 10.1007/BF00569125 (1986).

**142.** Araújo, P. G., Ribeiro, A. L. N., Yokoya, N. S. & Fujii, M. T. Temperature and salinity responses of drifting specimens of *Kappaphycus alvarezii* (Gigartinales, Rhodophyta) farmed on the Brazilian tropical coast. *J. applied phycology* **26**, 1979–1988, DOI: 10.1007/s10811-014-0303-9 (2014).

**143.** .

**144.** Terada, R. *et al.* The effect of irradiance and temperature on the photosynthesis and growth of a cultivated red alga *Kappaphycus alvarezii* (Solieriaceae) from Vietnam, based on in situ and in vitro measurements. *J. applied phycology* **28**, 457–467, DOI: 10.1007/s10811-015-0557-x (2016).

**145.** HARAGUCHI, H., MURASE, N., IMOTO, Z. & OKUDA, K. Culture and field studies on the temperature related growth rates of a tropical *Sargassum* species, *Sargassum* ilicifolium (Tuner) C. Agardh in Kochi Prefecture, southwestern Japan. *Algal Resour.* **11**, 1–10 (2018).

**146.** Zou, X.-X. *et al.* The effects of temperature, salinity and irradiance upon the growth of *Sargassum polycystum* C. Agardh (*Phaeophyceae*). *J. Appl. Phycol.* **30**, 1207–1215, DOI: 10.1007/s10811-017-1282-4 (2018).

**147.** Yamamoto, M., Watanabe, Y. & Kinoshita, H. Effects of water temperature on the growth of red alga *Porphyra yezoensis* form narawaensis (nori) cultivated in an outdoor raceway tank. *Nippon. Suisan Gakkaishi* **57**, 2211–2217 (1991).

**148.** Fernández, P. A. *et al.* Nitrogen sufficiency enhances thermal tolerance in habitat-forming kelp: implications for acclimation under thermal stress. *Sci. reports* **10**, 1–12, DOI: 10.1038/s41598-020-60104-4 (2020).

**149.** Zimmerman, R. C. & Kremer, J. N. In situ growth and chemical composition of the giant kelp, *Macrocystis pyrifera*: response to temporal changes in ambient nutrient availability. *Mar. Ecol. Prog. Ser.* **27**, 277–285 (1986).

## Acknowledgements

This work was funded by the ClimateWorks Foundation (UCI-21-1763). Additionally K.D. was supported by DOE/ARPA-E grant DE-AR0000920. We also appreciate the information provided by Dr. Loretta Roberson (MBL) through personal communication.

## Author contributions statement

K.A.D., C.F., B.S., and S.D. conceived the work. I.B.A.S. wrote the first draft off the manuscript. I.B.A.S., C.F., and B.S. designed and coded G-MACMODS, with the help of K.A.D. B.S. downloaded and interpolated the environmental forcing data. M.L. provided the nutrient data. M.L., S.D., and J.D. provided context for the atmospheric and economic implications of the work. All authors contributed to interpreting the results, as well as framing and revising the paper.

# Biophysical potential and uncertainties of global seaweed farming - Supplementary Material

**Isabella B. Arzeno-Soltero[1,*], Christina Frieder[2], Benjamin Saenz[3], Matthew Long[4], Julianne DeAngelo[5], Steven J. Davis[5,1], and Kristen Davis[1,5,*]**

[1]Department of Civil and Environmental Engineering, UC Irvine, Irvine, CA
[2]Southern California Coastal Water Research Project, Costa Mesa, CA
[3]biota.earth, Berkeley, CA
[4]National Center for Atmospheric Research, Boulder, CO
[5]Department of Earth System Science, UC Irvine, Irvine, CA
[*]iarzeno@uci.edu,davis@uci.edu

## Supplementary Figures

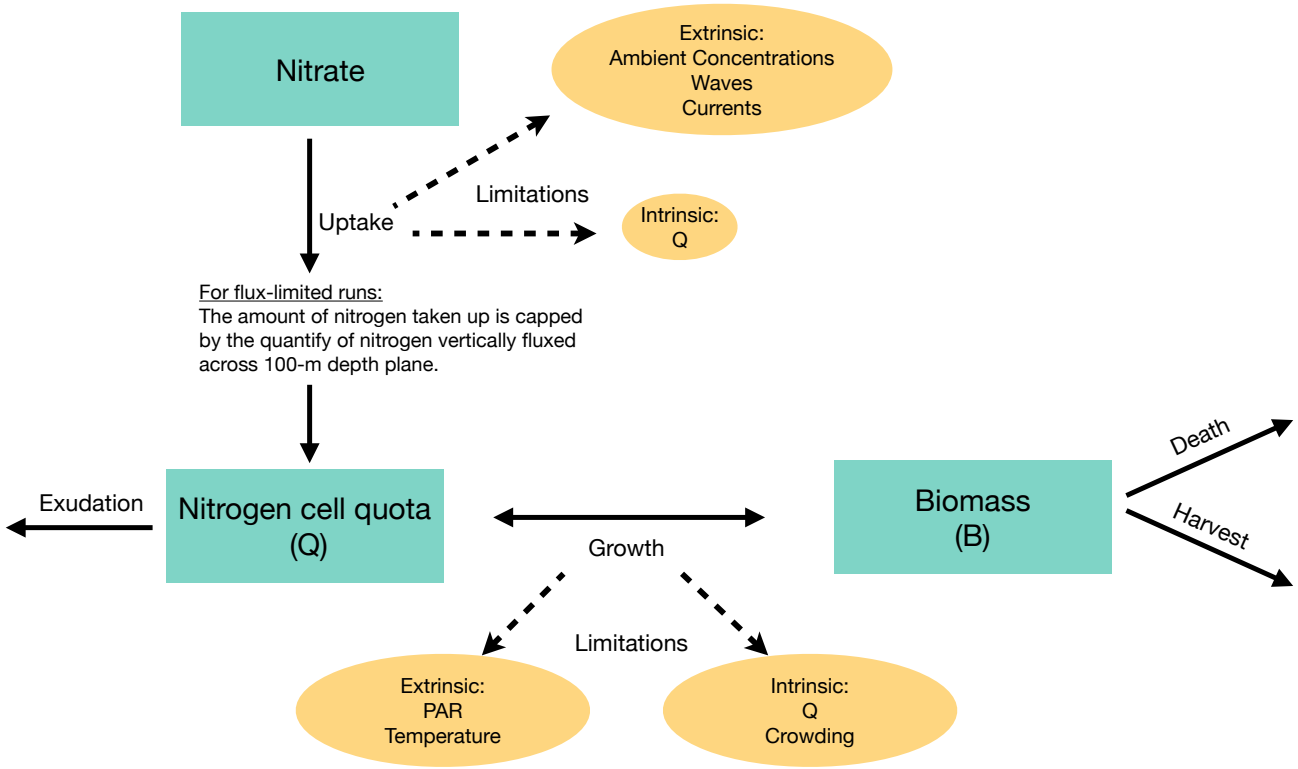


**Figure 1. Schematic overview of G-MACMODS**. For details, please refer to the Online Methods section of the manuscript.

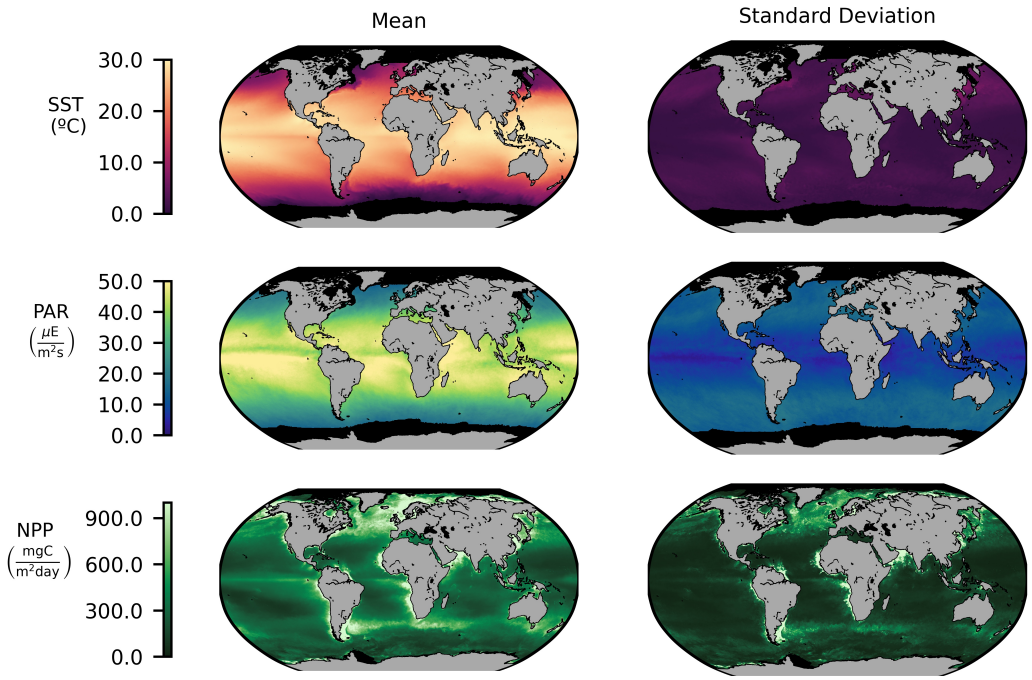


**Figure 2. Satellite-derived variables**. Temporal mean and standard deviation of the sea surface temperature (SST; top row), surface irradiance (PAR; middle row), and phytoplankton net primary productivity (NPP; bottom row) stemming from MODIS.

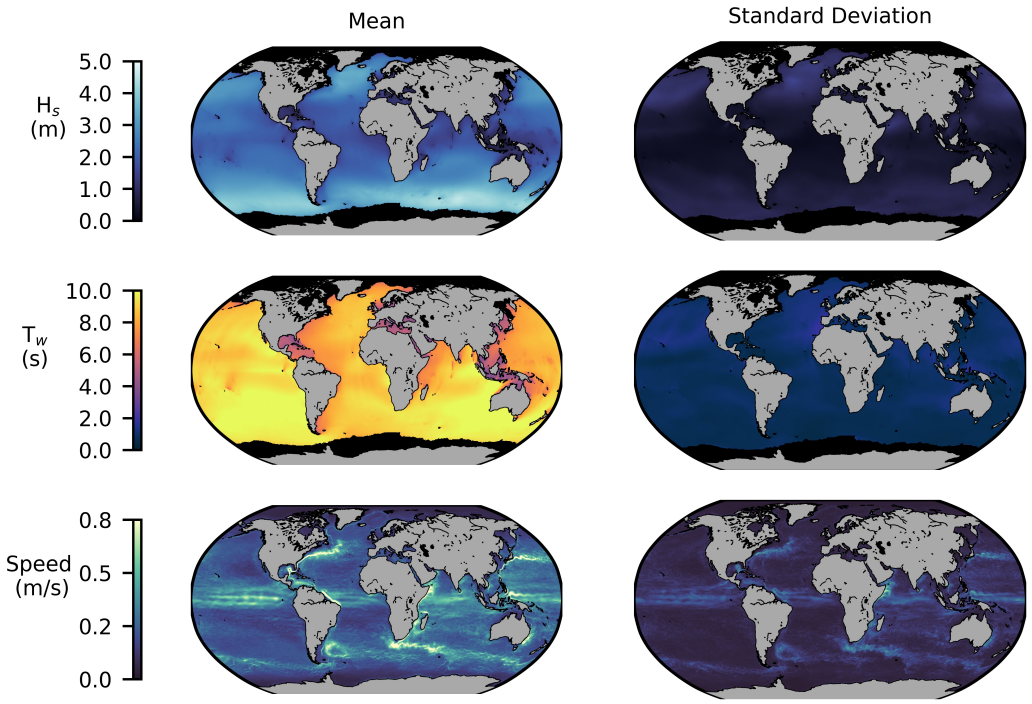


**Figure 3. Hydrodynamic variables**. Temporal mean and standard deviation of the significant wave height and mean wave period from ECMWF (top and middle row, respectively), as well as the surface current speed from HYCOM (bottom row).

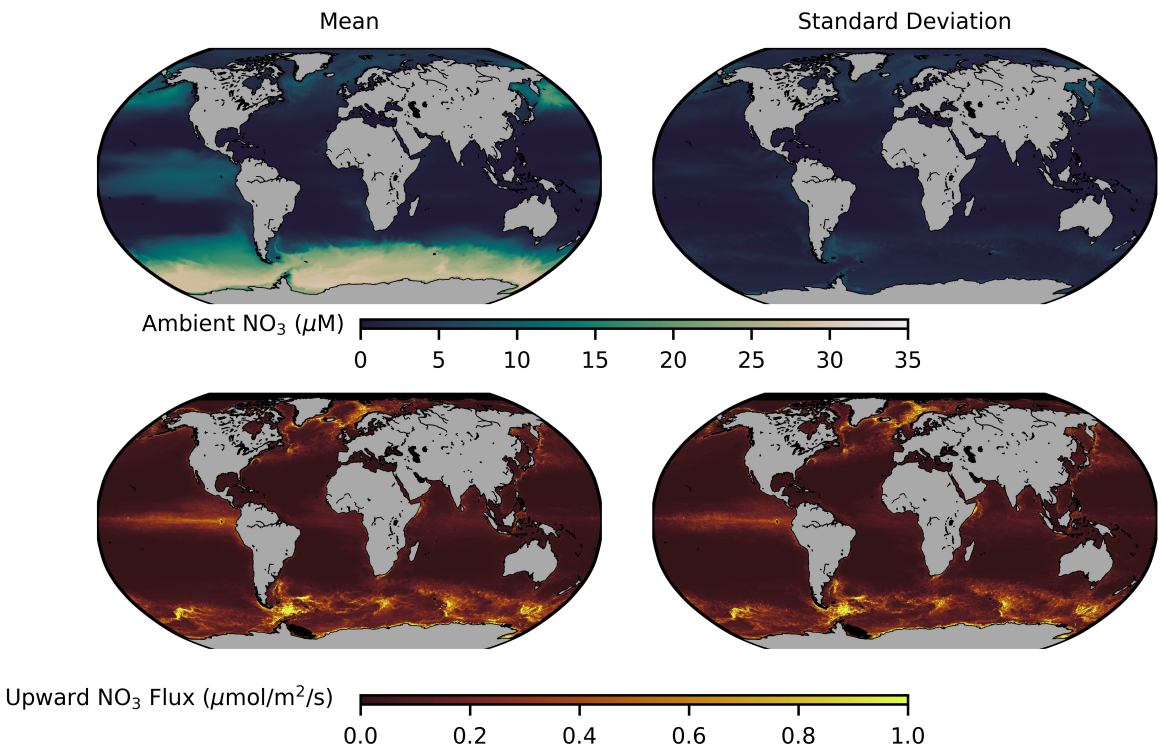


**Figure 4. CESM $NO_3$.** Temporal mean and standard deviation of the CESM depth-average ambient $NO_3$ concentrations (top row) and $NO_3$ flux across the 100-m depth plane (bottom row).

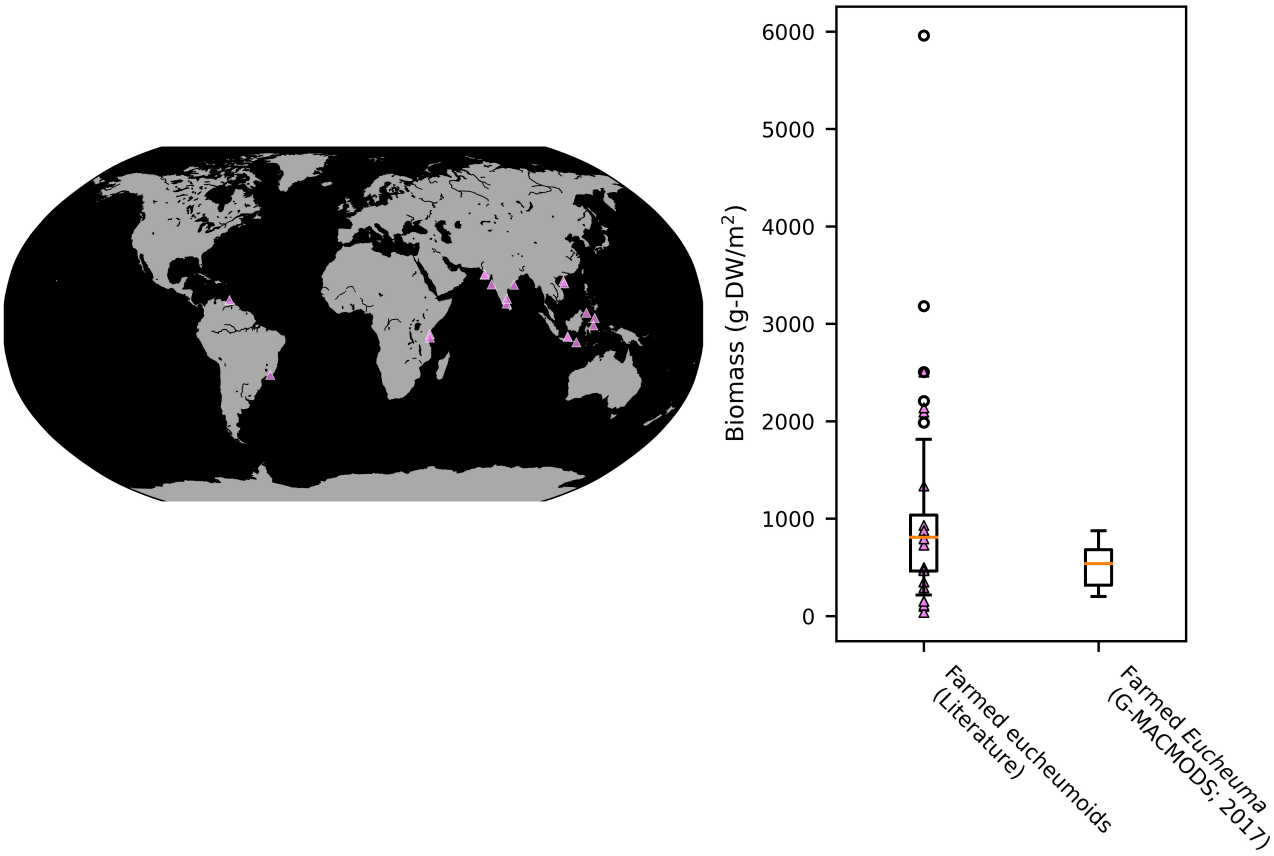


**Figure 5. Model-field comparisons (tropical red seaweed).** Locations of farmed *Eucheuma* and *Kappaphycus* observations in 1–19 (left panel). Some neighboring locations may not be resolved (may be plotted on top of other locations). Boxplots of *Eucheuma* and *Kappaphycus* harvest in 1–19, as well as the maximum tropical red seaweed biomass harvested in a single harvest cycle in G-MACMODS ambient nutrient simulations (right panel). Only values above B = 200 g-DW/m$^2$ (the tropical red seed weight in G-MACMODS) are shown in the boxplots (n = 74 values from 19 articles and > 600,000 values from G-MACMODS). Pink triangles indicate the mean harvest value in the literature articles referenced above. Values reported in fresh weight were converted to dry weight by assuming a dry-to-wet biomass ratio of 1:10.

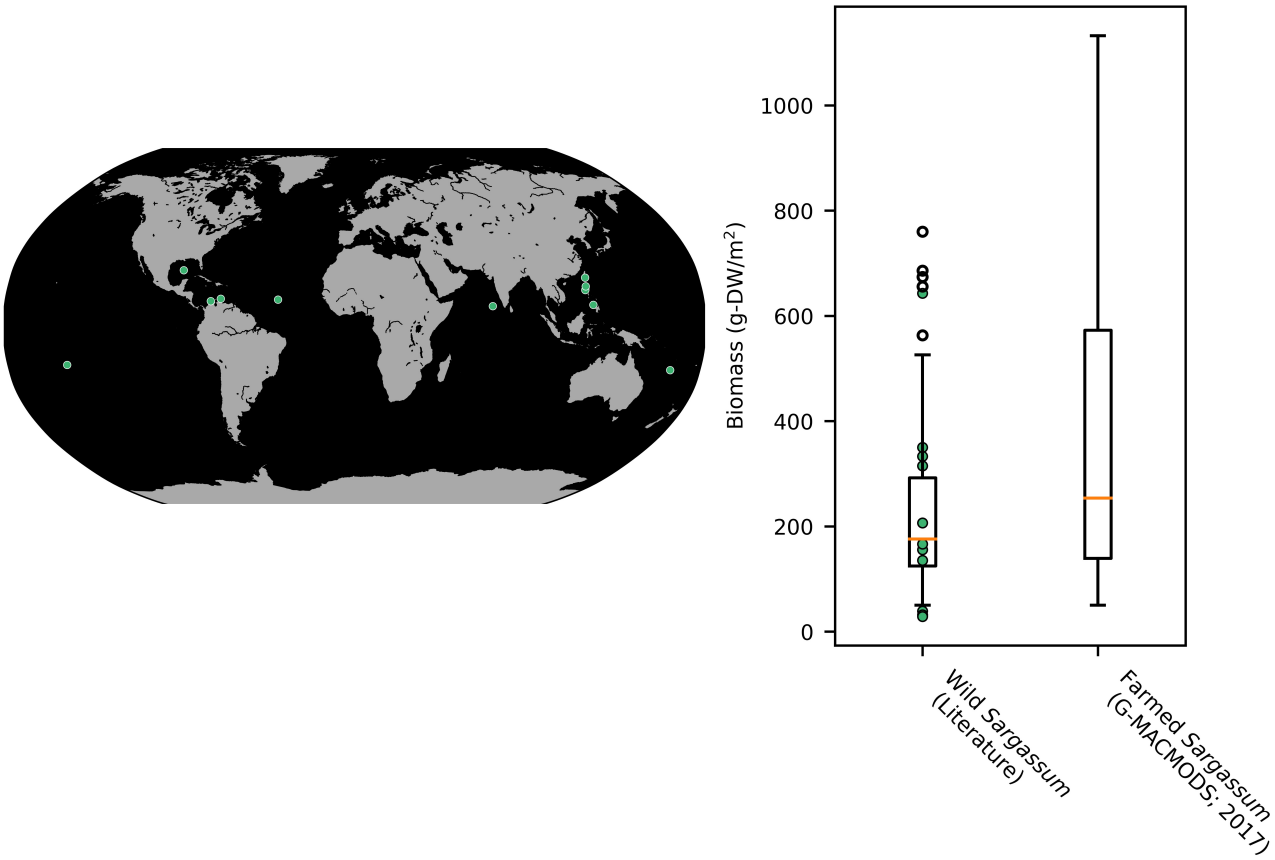


**Figure 6. Model-field comparisons (tropical brown seaweed).** Locations of wild *Sargassum* observations in 20–30 (left panel). Boxplots of wild *Sargassum* standing stock in 20–30, as well as the maximum tropical brown biomass observed in G-MACMODS ambient nutrient simulations when harvest is not imposed (to better match the wild seaweed values in the literature) are shown in the right panel. Only values above B = 50 g-DW/m$^2$ (the tropical brown seed weight in G-MACMODS) are shown in the boxplots (n = 40 values from 10 articles and > 900,000 values from G-MACMODS). Green circles indicate the mean reported biomass in the literature articles referenced above. Values reported in fresh weight were converted to dry weight by assuming a dry-to-wet biomass ratio of 1:10.

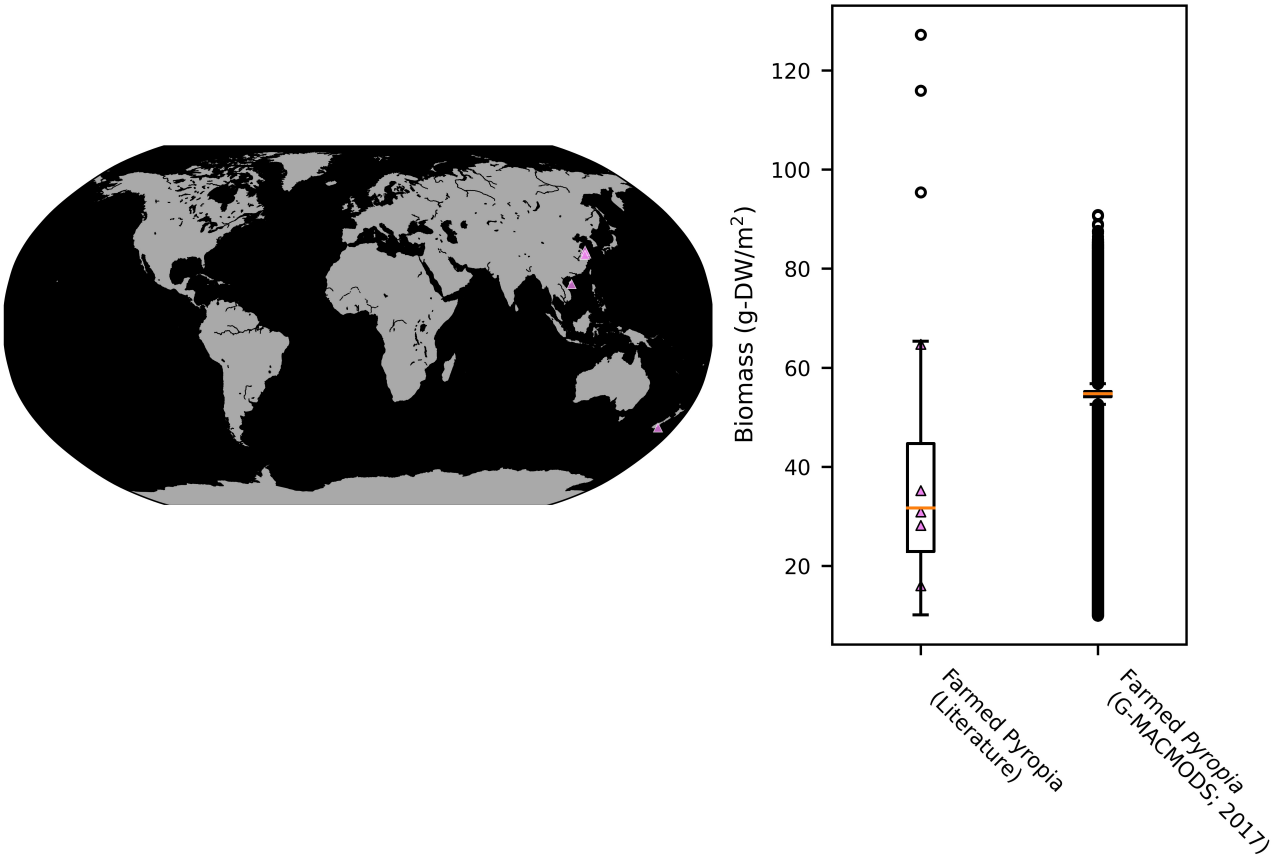


**Figure 7. Model-field comparisons (temperate red seaweed).** Locations of farmed *Pyropia* observations in 7, 12, 31–33 (left panel). Boxplots of *Pyropia* harvest in 7, 12, 31–33, as well as the maximum temperate red seaweed biomass harvested in a single harvest cycle in G-MACMODS ambient nutrient simulations (right panel). Only values above B = 10 g-DW/m$^2$ (the temperate red seed weight in G-MACMODS) are shown in the boxplots (n = 53 values from 5 articles and > 1.8 million values from G-MACMODS). Pink triangles indicate the mean harvest values in the literature articles referenced above. Values reported in fresh weight were converted to dry weight by assuming a dry-to-wet biomass ratio of 1:10.

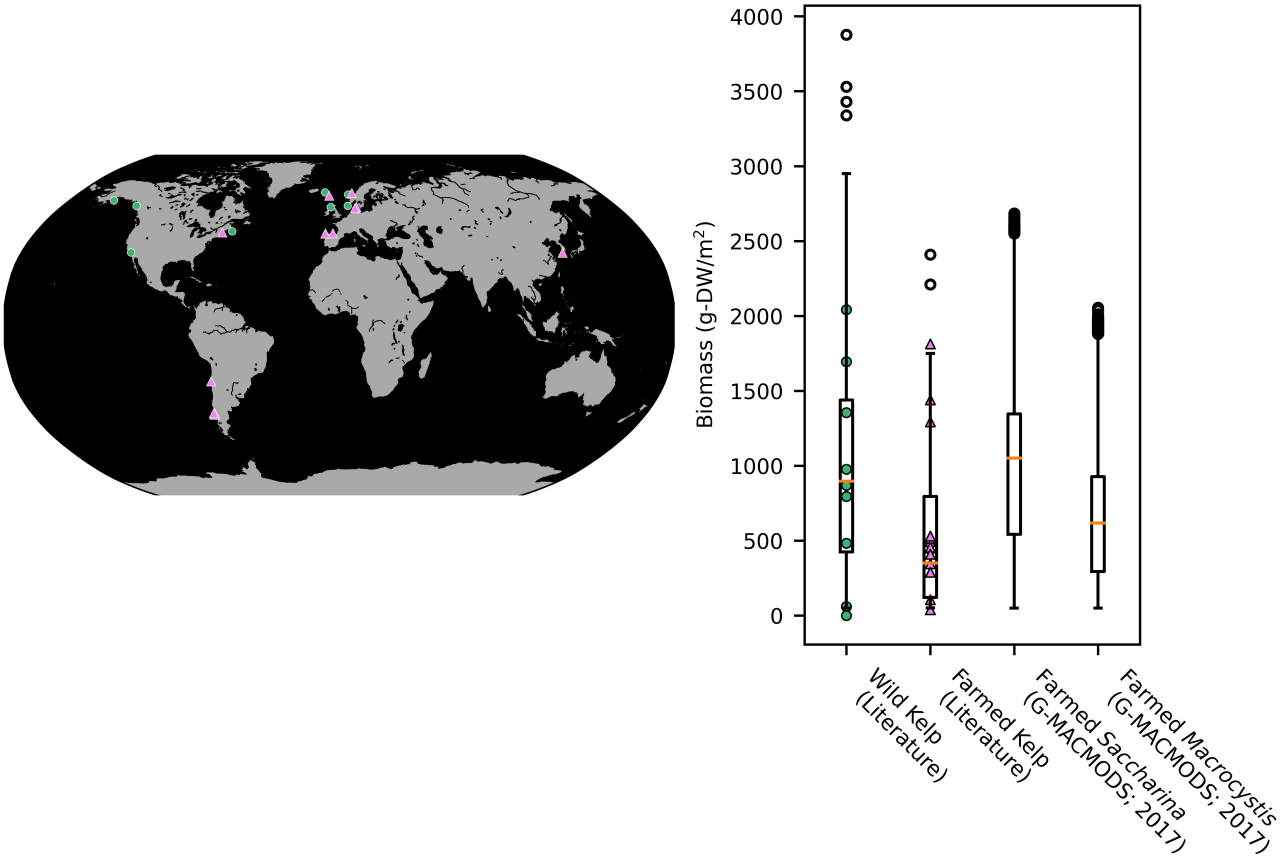


**Figure 8. Model-field comparisons (temperate brown seaweed).** Locations of wild (34–43; green circles) and farmed (44–56; pink triangles) *Saccharina*, *Laminaria*, and *Macrocystis* observations (left panel). Some neighboring locations may not be resolved (may be plotted on top of other locations). Boxplots of wild standing stock values from 34–43 (n = 127 values from 10 articles), harvest from 44–56 (n = 80 values from 13 articles), and maximum kelp biomass output from G-MACMODS (ambient nutrient scenario) when harvest is not imposed (n > 1.5 million values) are showin in the right panel. Only values above B = 50 g-DW/m$^2$ (the temperate brown seed weight in G-MACMODS) are shown in the boxplots. Green circles and pink triangles indicate the mean reported biomass in the literature articles that discuss wild and farmed kelp, respectively. Values reported in fresh weight were converted to dry weight by assuming a dry-to-wet biomass ratio of 1:10.

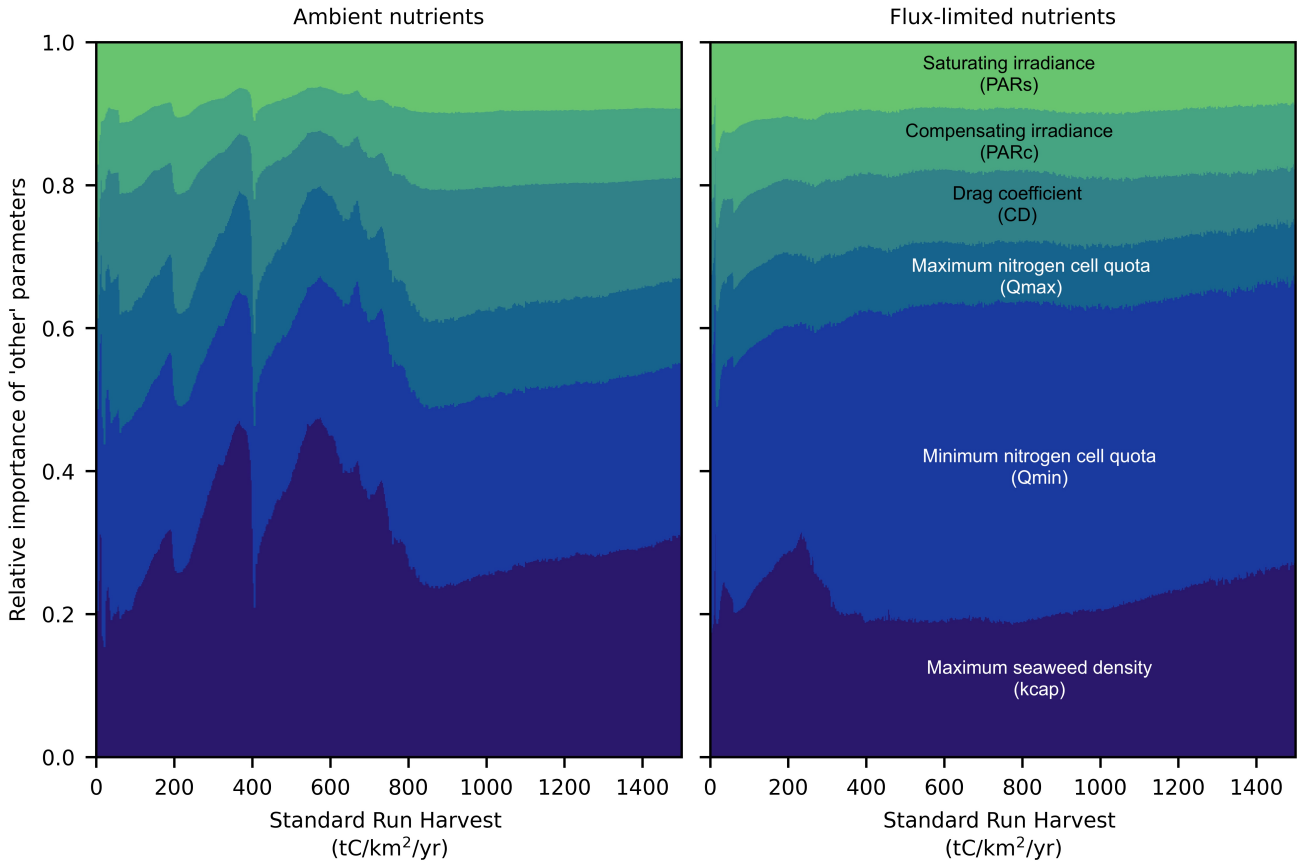


**Figure 9. Random forest results.** Focused view of the "other" category in Figure 3 of the main manuscript. The results have been normalized to reflect the relative importance of each parameter. For parameter information, please refer to Table 1 of the main manuscript.

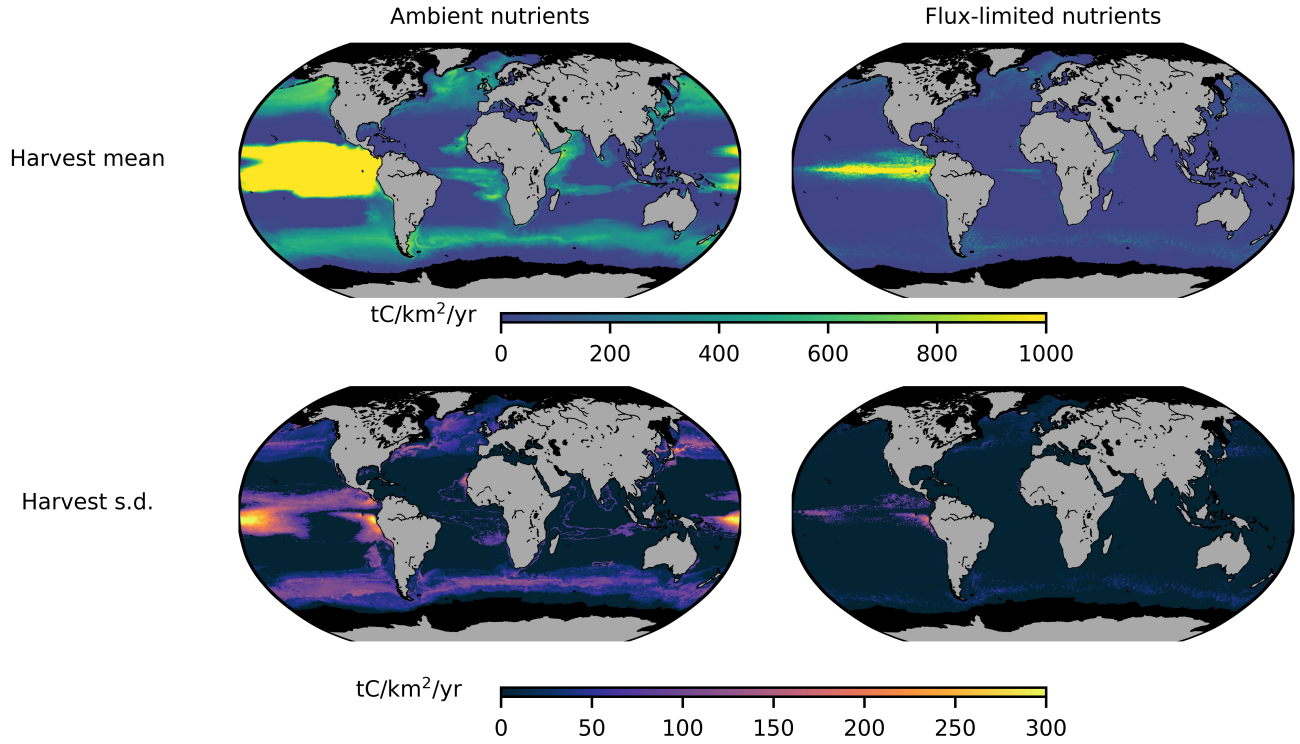


**Figure 10. Inter-annual harvest variability**. Harvest yield temporal mean (top row) and standard deviation (bottom row) across 2002–2019.

## References


1. Wakibia, J., Ochiewo, J. & Bolton, J. J. Economic analysis of eucheumoid algae farming in Kenya. *West. Indian Ocean. J. Mar. Sci.* **10**, 13–24 (2011).
2. Nugroho, R., Wijayanto, D., Kurohman, F., Maulina, I. & Puspitasari, R. The Growth Analysis of Euchema *cottonii* using The Simple Longline Method and Basket Method on The Coast of Kemojan Island. In *IOP Conference Series: Earth and Environmental Science*, vol. 750, 012056, DOI: 10.1088/1755-1315/750/1/012056 (IOP Publishing, 2021).
3. Periyasamy, C., Rao, P. S. & Anantharaman, P. Harvest optimization to assess sustainable growth and carrageenan yield of cultivated *Kappaphycus alvarezii* (Doty) Doty in Indian waters. *J. Appl. Phycol.* **31**, 587–597, DOI: 10.1007/s10811-018-1562-7 (2019).
4. Villanueva, R. D., Romero, J. B., Montaño, M. N. E. & Purita, O. Harvest optimization of four *Kappaphycus* species from the Philippines. *Biomass bioenergy* **35**, 1311–1316, DOI: 10.1016/j.biombioe.2010.12.044 (2011).
5. de Góes, H. G. & Reis, R. P. An initial comparison of tubular netting versus tie–tie methods of cultivation for *Kappaphycus alvarezii* (Rhodophyta, Solieriaceae) on the south coast of Rio de Janeiro State, Brazil. *J. Appl. Phycol.* **23**, 607–613, DOI: 10.1007/s10811-010-9647-y (2011).
6. Kumar, K. S., Ganesan, K., Rao, P. S. & Thakur, M. Seasonal studies on field cultivation of *Kappaphycus alvarezii* (Doty) Doty on the northwest coast of India. *J. applied phycology* **28**, 1193–1205, DOI: 10.1007/s10811-015-0629-y (2016).
7. Wang, X. *et al.* Economically important red algae resources along the Chinese coast: History, status, and prospects for their utilization. *Algal Res.* **46**, 101817, DOI: 10.1016/j.algal.2020.101817 (2020).
8. Juanich, G. L. Manual on seaweed farming 1. *Eucheuma* spp. (1988).
9. Ndobe, S. *et al.* *Eucheuma*toid seaweed farming under global change-Tomini Bay seaweed trial indicates *Eucheuma* denticulatum (spinosum) could contribute to climate adaptation. *Aquac. Aquarium, Conserv. & Legislation* **13**, 2452–2467 (2020).
10. Msuya, F. E. *et al.* A comparative economic analysis of two seaweed farming methods in Tanzania. *The Sustain. Coast. Communities Ecosyst. Program. Coast. Resour. Center, Univ. Rhode Island West. Indian Ocean. Mar. Sci. Assoc.* (2007).
11. Ganesan, M. *et al.* Seaweed resources in India–current status of diversity and cultivation: prospects and challenges. *Bot. Mar.* **62**, 463–482, DOI: 10.1515/bot-2018-0056 (2019).
12. Hwang, E. K., Yotsukura, N., Pang, S. J., Su, L. & Shan, T. F. Seaweed breeding programs and progress in eastern Asian countries. *Phycologia* **58**, 484–495, DOI: 10.1080/00318884.2019.1639436 (2019).
13. Hurtado, A. Q. Social and economic dimensions of carrageenan seaweed farming in the Philippines. *Soc. Econ. Dimensions Carrageenan Seaweed Farming. Fish. Aquac. Tech. Pap. No. 580* (2013).
14. Neish, I. C. Social and economic dimensions of carrageenan seaweed farming in Indonesia. *Soc. Econ. Dimensions Carrageenan Seaweed Farming. Fish. Aquac. Tech. Pap. No. 580* (2013).
15. Periyasamy, C. & Rao, P. S. Growth rate and carrageenan yield of cultivated *Kappaphycus alvarezii* (Doty) Doty in the coastal waters of Bay of Bengal at Chepala Timmapuram, Andhra Pradesh, east coast of India. *J. Appl. Phycol.* **29**, 1977–1987, DOI: 10.1007/s10811-017-1099-1 (2017).
16. Wijayanto, D., Bambang, A. N., Nugroho, R. A. & Kurohman, F. The impact of planting distance on productivity and profit of *Eucheuma cottonii* seaweed cultivation in Karimunjawa Islands, Indonesia. *Aquac. Aquarium, Conserv. & Legislation* **13**, 2170–2179 (2020).
17. Thirumaran, G. & Anantharaman, P. Daily Growth Rate of Field Farming Seaweed *Kappaphycus alvarezii* (Doty) Doty ex. P. Silva in Vellar Estuary. *World J. Fish Mar. Sci.* **1**, 144–153 (2009).
18. Rosas, E. D. V. M., Cabrera, J. A. R., León, R. E. R. & Rodríguez, J. L. N. Evaluación del crecimiento de *Eucheuma isiforme* (Rhodophyta, Gigartinales) en sistemas de cultivo suspendidos en la isla de Cubagua, Venezuela (sureste del Mar Caribe). *AquaTechnica: Revista Iberoamericana de Acuicultura.* **2**, 86–98 (2020).
19. Makwana, N. P. Growth comparison of the seaweed *Kappaphycus alvarezii* in nine different coastal areas of Gujarat coast, India. *Adv. Appl. Sci. Res.* **2**, 99–106 (2011).
20. Trono Jr, G. C. & Tolentino, G. L. Studies on the management of *Sargassum* (Fucales, Phaeophyta) bed in Bolinao, Pangasinan, Philippines. *The Korean J. Phycol.* **8**, 249–257 (1993).
21. Rani, V., Jawahar, P. & Jeya Shakila, R. Seasonal variation in biomass and distribution of brown seaweeds (Phaeophyceae) in Gulf of Mannar, Tamilnadu, India. *The Bioscan* **10**, 1123–1129 (2015).

**22.** .

**23.** Ody, A. *et al.* From In Situ to satellite observations of pelagic *Sargassum* distribution and aggregation in the Tropical North Atlantic Ocean. *PLoS One* **14**, e0222584, DOI: 10.1371/journal.pone.0222584 (2019).

**24.** Engelen, A. H., Åberg, P., Olsen, J. L., Stam, W. T. & Breeman, A. M. Effects of wave exposure and depth on biomass, density and fertility of the fucoid seaweed *Sargassum polyceratium* (Phaeophyta, Sargassaceae). *Eur. J. Phycol.* **40**, 149–158, DOI: 10.1080/09670260500109210 (2005).

**25.** Camacho, O. & Hernández-Carmona, G. Phenology and alginates of two *Sargassum* species from the Caribbean coast of Colombia. *Ciencias Mar.* **38**, 381–393 (2012).

**26.** Andrefouet, S., Zubia, M. & Payri, C. Mapping and biomass estimation of the invasive brown algae Turbinaria ornata (Turner) J. Agardh and *Sargassum mangarevense* (Grunow) Setchell on heterogeneous Tahitian coral reefs using 4-meter resolution IKONOS satellite data. *Coral Reefs* **23**, 26–38, DOI: 10.1007/s00338-003-0367-5 (2004).

**27.** Mattio, L., Payri, C. E. & Stiger-Pouvreau, V. Taxonomic revision of *Sargassum* (Fucales, Phaeophycae) from French Polynesia based on Morphological and MOlecular Analyses 1. *J. phycology* **44**, 1541–1555, DOI: 10.1111/j.1529-8817.2008.00597.x (2008).

**28.** Calumpong, H., Maypa, A. & Magbanua, M. Population and alginate yield and quality assessment of four *Sargassum* species in Negros Island, central Philippines. *Hydrobiologia* **398**, 211–215, DOI: 10.1023/A:1017015824822 (1999).

**29.** Hwang, R.-L., Tsai, C.-C. & Lee, T.-M. Assessment of temperature and nutrient limitation on seasonal dynamics among species of *Sargassum* from a coral reef in Southern Taiwan 1. *J. Phycol.* **40**, 463–473, DOI: doi.org/10.1111/j.1529-8817.2004.03086.x (2004).

**30.** Wang, M. *et al.* The great Atlantic *Sargassum* belt. *Science* **365**, 83–87, DOI: 10.1126/science.aaw7912 (2019).

**31.** He, P. *et al.* Bioremediation efficiency in the removal of dissolved inorganic nutrients by the red seaweed, *Porphyra yezoensis*, cultivated in the open sea. *Water Res.* **42**, 1281–1289, DOI: 10.1016/j.watres.2007.09.023 (2008).

**32.** Wu, H., Kim, J. K., Huo, Y., Zhang, J. & He, P. Nutrient removal ability of seaweeds on *Pyropia yezoensis* aquaculture rafts in China's radial sandbanks. *Aquatic Bot.* **137**, 72–79, DOI: 10.1016/j.aquabot.2016.11.011 (2017).

**33.** O'Connell-Milne, S. A. & Hepburn, C. D. A harvest method informed by traditional knowledge maximises yield and regeneration post harvest for karengo (Bangiaceae). *J. applied phycology* **27**, 447–454, DOI: 10.1007/s10811-014-0318-2 (2015).

**34.** Krumhansl, K. A. & Scheibling, R. E. Detrital production in Nova Scotian kelp beds: patterns and processes. *Mar. Ecol. Prog. Ser.* **421**, 67–82, DOI: 10.3354/meps08905 (2011).

**35.** Gundersen, H. *et al.* Variation in Population Structure and Standing Stocks of Kelp Along Multiple Environmental Gradients and Implications for Ecosystem Services. *Front. Mar. Sci.* **8**, 360, DOI: 10.3389/fmars.2021.578629 (2021).

**36.** van Son, T. C. *et al.* Achieving reliable estimates of the spatial distribution of kelp biomass. *Front. Mar. Sci.* **7**, 107, DOI: 10.3389/fmars.2020.00107 (2020).

**37.** Smale, D. A. *et al.* Linking environmental variables with regional-scale variability in ecological structure and standing stock of carbon within UK kelp forests. *Mar. Ecol. Prog. Ser.* **542**, 79–95, DOI: 10.3354/meps11544 (2016).

**38.** Ulaski, B. P., Konar, B. & Otis, E. O. Seaweed Reproduction and Harvest Rebound in Southcentral Alaska: Implications for Wild Stock Management. *Estuaries Coasts* **43**, 2046–2062, DOI: 10.1007/s12237-020-00740-1 (2020).

**39.** Rassweiler, A., Reed, D. C., Harrer, S. L. & Nelson, J. C. Improved estimates of net primary production, growth, and standing crop of *Macrocystis pyrifera* in Southern California, DOI: 10.1002/ecy.2440 (2018).

**40.** Muraoka, D. Seaweed resources as a source of carbon fixation. *Bull. research agency Jpn.* 59–64 (2004).

**41.** Stekoll, M., Deysher, L. & Hess, M. A remote sensing approach to estimating harvestable kelp biomass. In *Eighteenth International Seaweed Symposium*, 97–108, DOI: 10.1007/978-1-4020-5670-3_13 (Springer, 2006).

**42.** Pedersen, M. F., Nejrup, L. B., Fredriksen, S., Christie, H. & Norderhaug, K. M. Effects of wave exposure on population structure, demography, biomass and productivity of the kelp Laminaria hyperborea. *Mar. Ecol. Prog. Ser.* **451**, 45–60, DOI: 10.3354/meps09594 (2012).

**43.** Pessarrodona, A., Moore, P. J., Sayer, M. D. & Smale, D. A. Carbon assimilation and transfer through kelp forests in the NE Atlantic is diminished under a warmer ocean climate. *Glob. Chang. Biol.* **24**, 4386–4398, DOI: 10.1111/gcb.14303 (2018).

**44.** Forbord, S., Steinhovden, K. B., Solvang, T., Handå, A. & Skjermo, J. Effect of seeding methods and hatchery periods on sea cultivation of *Saccharina latissima* (Phaeophyceae): a Norwegian case study. *J. Appl. Phycol.* **32**, 2201–2212, DOI: 10.1007/s10811-019-01936-0 (2020).

**45.** Freitas, J. R., Morrondo, J. M. S. & Ugarte, J. C. *Saccharina latissima* (Laminariales, Ochrophyta) farming in an industrial IMTA system in Galicia (Spain). *J. applied phycology* **28**, 377–385, DOI: 10.1007/s10811-015-0526-4 (2016).

**46.** Augyte, S., Yarish, C., Redmond, S. & Kim, J. K. Cultivation of a morphologically distinct strain of the sugar kelp, *Saccharina latissima* forma angustissima, from coastal Maine, USA, with implications for ecosystem services. *J. Appl. Phycol.* **29**, 1967–1976, DOI: 10.1007/s10811-017-1102-x (2017).

**47.** Boderskov, T. *et al.* Effects of seeding method, timing and site selection on the production and quality of sugar kelp, *Saccharina latissima*: A Danish case study. *Algal Res.* **53**, 102160, DOI: 10.1016/j.algal.2020.102160 (2021).

**48.** Park, C. S. & Hwang, E. K. Seasonality of epiphytic development of the hydroid Obelia geniculata on cultivated *Saccharina japonica* (Laminariaceae, Phaeophyta) in Korea. *J. applied phycology* **24**, 433–439, DOI: 10.1007/s10811-011-9755-3 (2012).

**49.** Bak, U. G., Mols-Mortensen, A. & Gregersen, O. Production method and cost of commercial-scale offshore cultivation of kelp in the Faroe Islands using multiple partial harvesting. *Algal research* **33**, 36–47, DOI: 10.1016/j.algal.2018.05.001 (2018).

**50.** Peteiro, C. & Freire, Ó. Biomass yield and morphological features of the seaweed *Saccharina latissima* cultivated at two different sites in a coastal bay in the Atlantic coast of Spain. *J. applied phycology* **25**, 205–213, DOI: 10.1007/s10811-012-9854-9 (2013).

**51.** Peteiro, C., Sánchez, N., Dueñas-Liaño, C. & Martínez, B. Open-sea cultivation by transplanting young fronds of the kelp *Saccharina latissima*. *J. applied phycology* **26**, 519–528, DOI: 10.1007/s10811-013-0096-2 (2014).

**52.** Marinho, G. S., Holdt, S. L., Birkeland, M. J. & Angelidaki, I. Commercial cultivation and bioremediation potential of sugar kelp, *Saccharina latissima*, in Danish waters. *J. applied phycology* **27**, 1963–1973, DOI: 10.1007/s10811-014-0519-8 (2015).

**53.** Macchiavello, J., Araya, E. & Bulboa, C. Production of *Macrocystis pyrifera* (Laminariales; Phaeophyceae) in northern Chile on spore-based culture. *J. Appl. Phycol.* **22**, 691–697, DOI: 10.1007/s10811-010-9508-8 (2010).

**54.** Correa, T. *et al.* Production and economic assessment of giant kelp *Macrocystis pyrifera* cultivation for abalone feed in the south of C hile. *Aquac. research* **47**, 698–707, DOI: 10.1111/are.12529 (2016).

**55.** Gutierrez, A. *et al.* Farming of the giant kelp *Macrocystis pyrifera* in southern Chile for development of novel food products. In *Eighteenth International Seaweed Symposium*, 33–41, DOI: 10.1007/978-1-4020-5670-3_5 (Springer, 2006).

**56.** Camus, C., Infante, J. & Buschmann, A. H. Overview of 3 year precommercial seafarming of *Macrocystis pyrifera* along the Chilean coast. *Rev. Aquac.* **10**, 543–559, DOI: 10.1111/raq.12185 (2018).

# Biophysical potential and uncertainties of global seaweed farming - Supplementary Material

**Isabella B. Arzeno-Soltero[1,*], Christina Frieder[2], Benjamin Saenz[3], Matthew Long[4], Julianne DeAngelo[5], Steven J. Davis[5,1], and Kristen Davis[1,5,*]**

[1]Department of Civil and Environmental Engineering, UC Irvine, Irvine, CA
[2]Southern California Coastal Water Research Project, Costa Mesa, CA
[3]biota.earth, Berkeley, CA
[4]National Center for Atmospheric Research, Boulder, CO
[5]Department of Earth System Science, UC Irvine, Irvine, CA
[*]iarzeno@uci.edu,davis@uci.edu

## Supplementary Figures

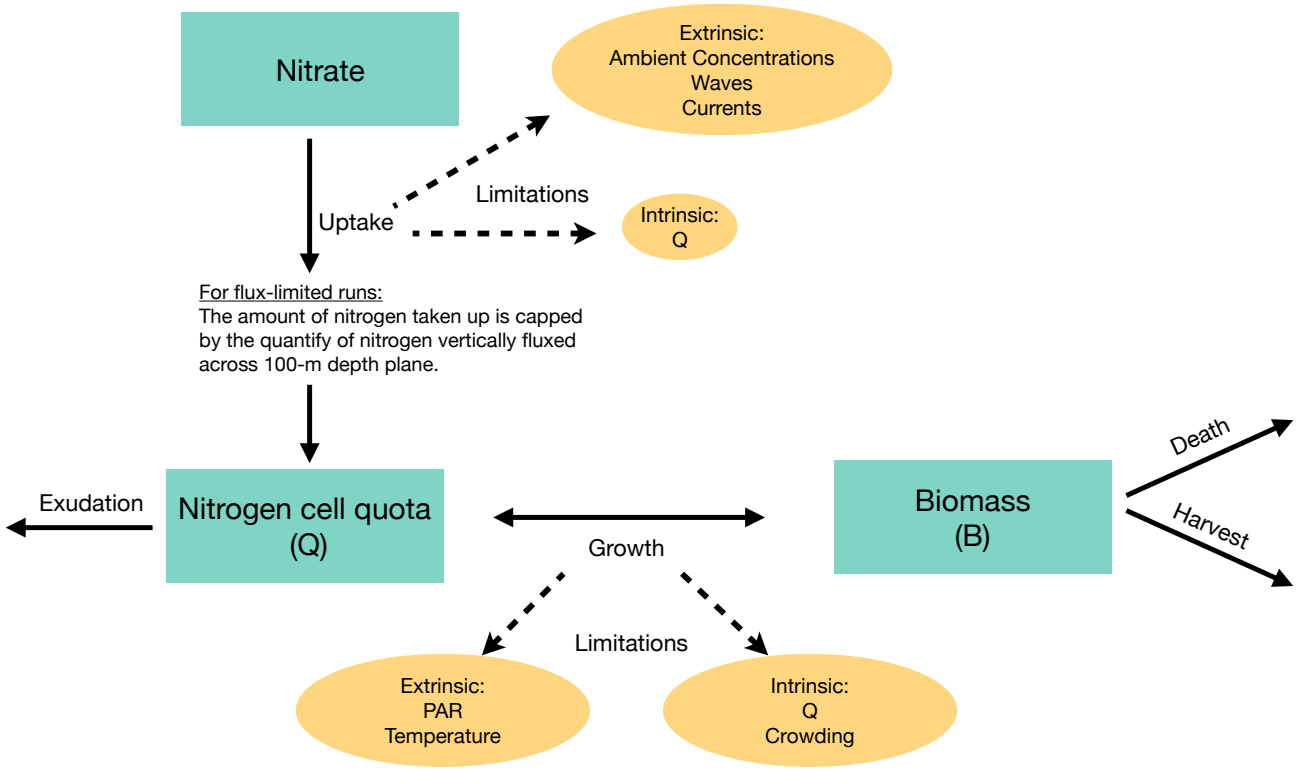


**Figure 1. Schematic overview of G-MACMODS**. For details, please refer to the Online Methods section of the manuscript.

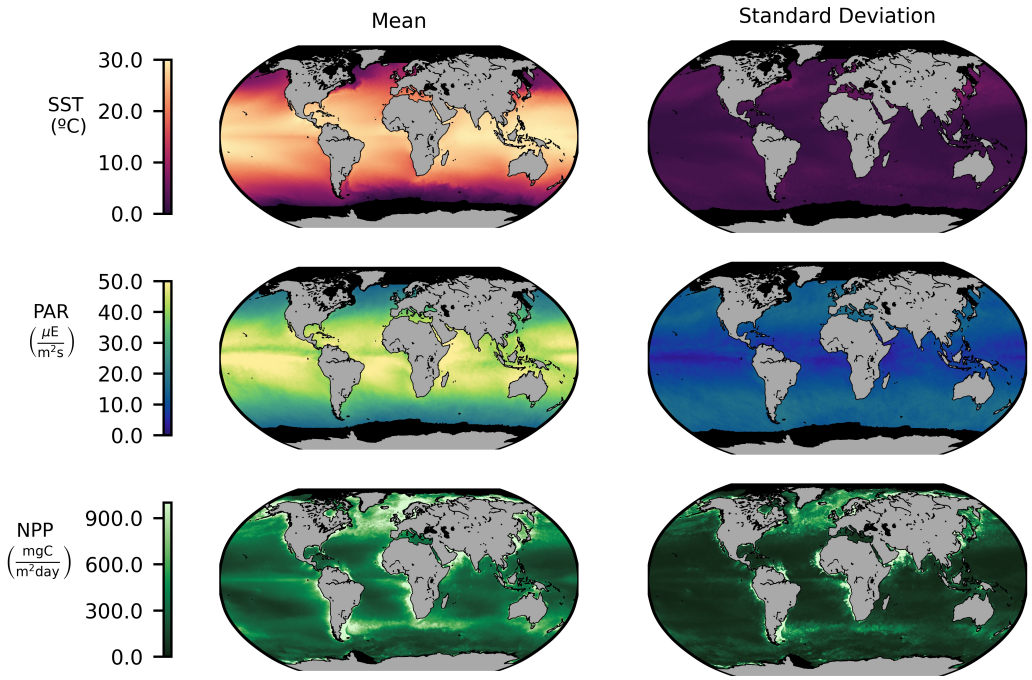


**Figure 2. Satellite-derived variables**. Temporal mean and standard deviation of the sea surface temperature (SST; top row), surface irradiance (PAR; middle row), and phytoplankton net primary productivity (NPP; bottom row) stemming from MODIS.

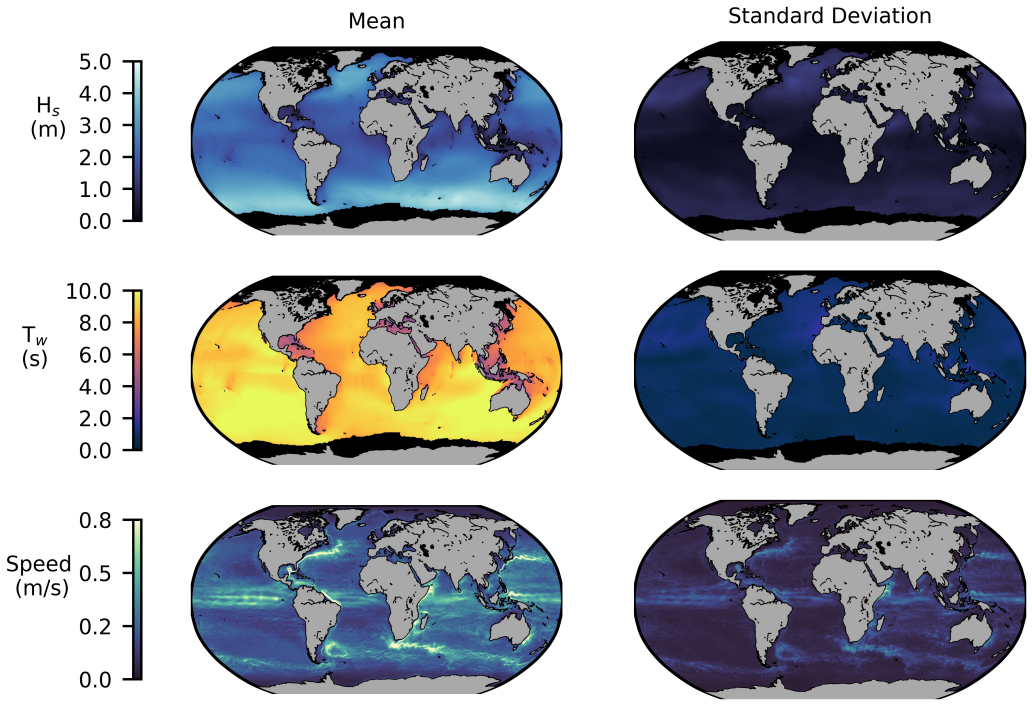


**Figure 3. Hydrodynamic variables**. Temporal mean and standard deviation of the significant wave height and mean wave period from ECMWF (top and middle row, respectively), as well as the surface current speed from HYCOM (bottom row).

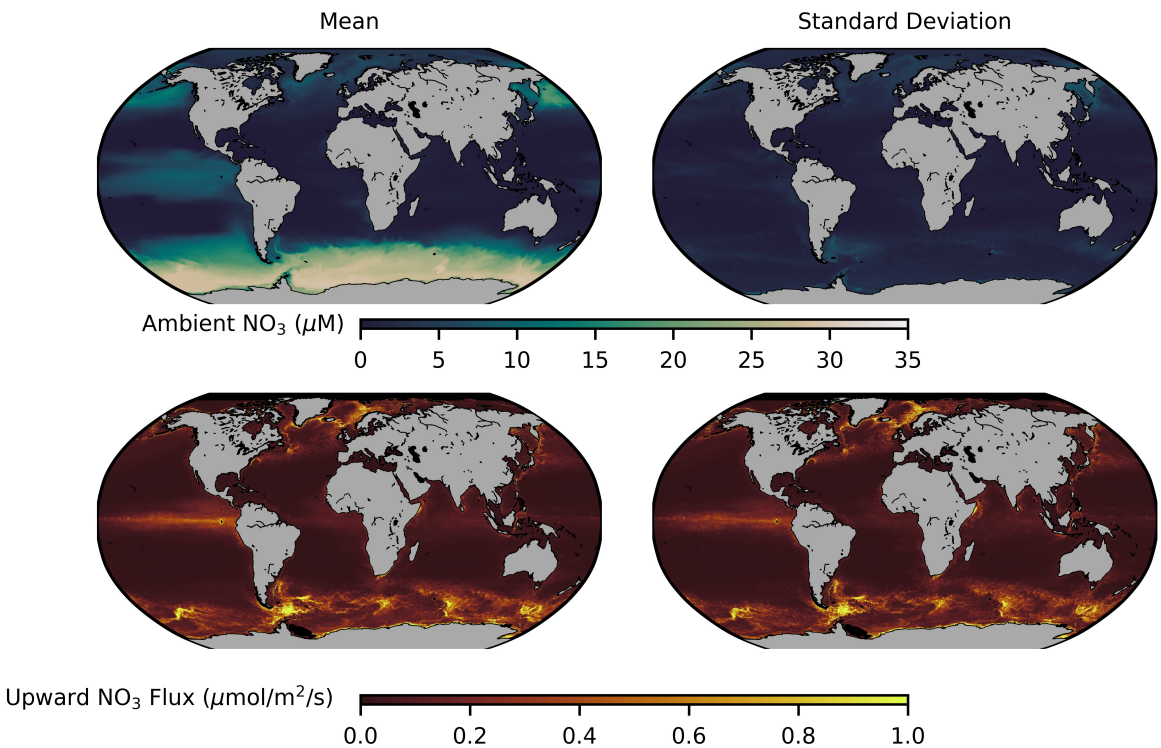


**Figure 4. CESM $NO_3$.** Temporal mean and standard deviation of the CESM depth-average ambient $NO_3$ concentrations (top row) and $NO_3$ flux across the 100-m depth plane (bottom row).

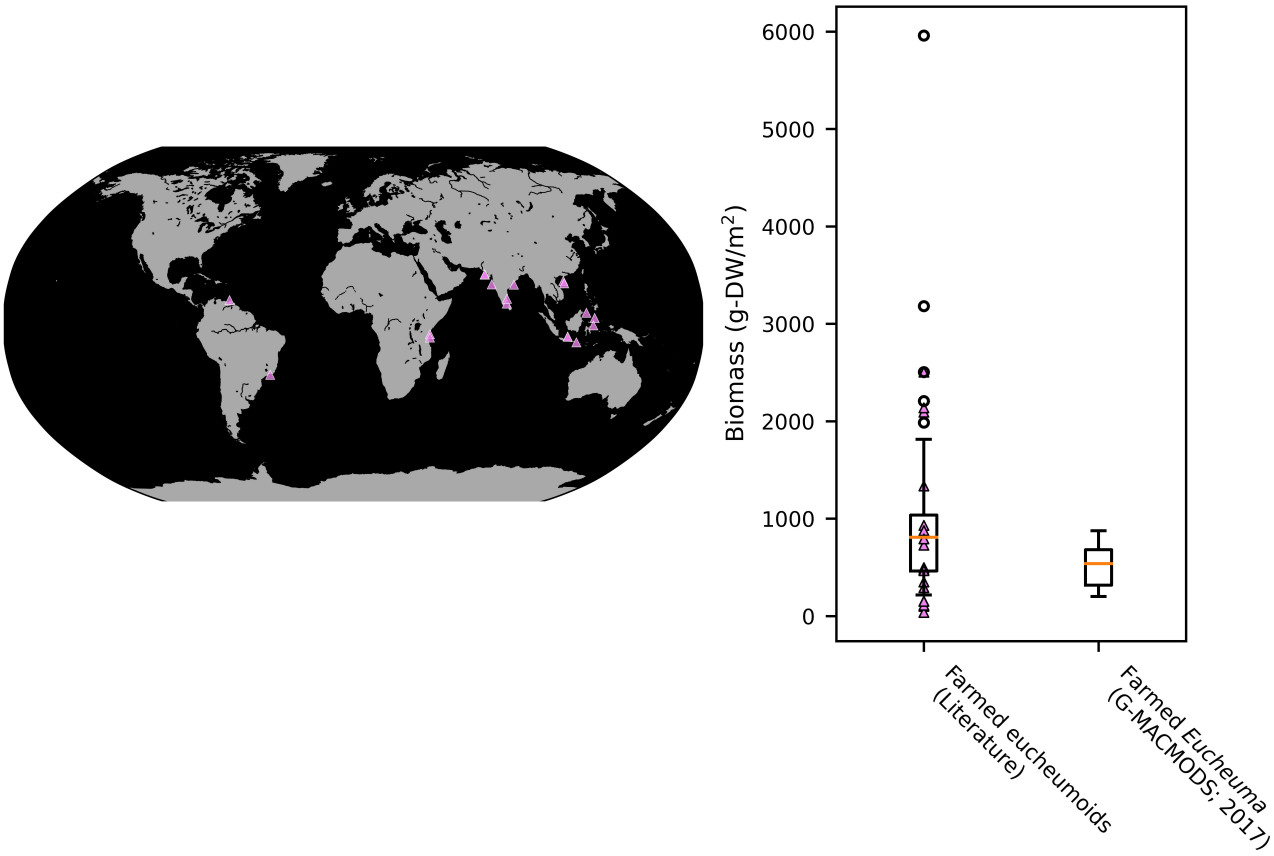


**Figure 5. Model-field comparisons (tropical red seaweed).** Locations of farmed *Eucheuma* and *Kappaphycus* observations in 1–19 (left panel). Some neighboring locations may not be resolved (may be plotted on top of other locations). Boxplots of *Eucheuma* and *Kappaphycus* harvest in 1–19, as well as the maximum tropical red seaweed biomass harvested in a single harvest cycle in G-MACMODS ambient nutrient simulations (right panel). Only values above B = 200 g-DW/m$^2$ (the tropical red seed weight in G-MACMODS) are shown in the boxplots (n = 74 values from 19 articles and > 600,000 values from G-MACMODS). Pink triangles indicate the mean harvest value in the literature articles referenced above. Values reported in fresh weight were converted to dry weight by assuming a dry-to-wet biomass ratio of 1:10.

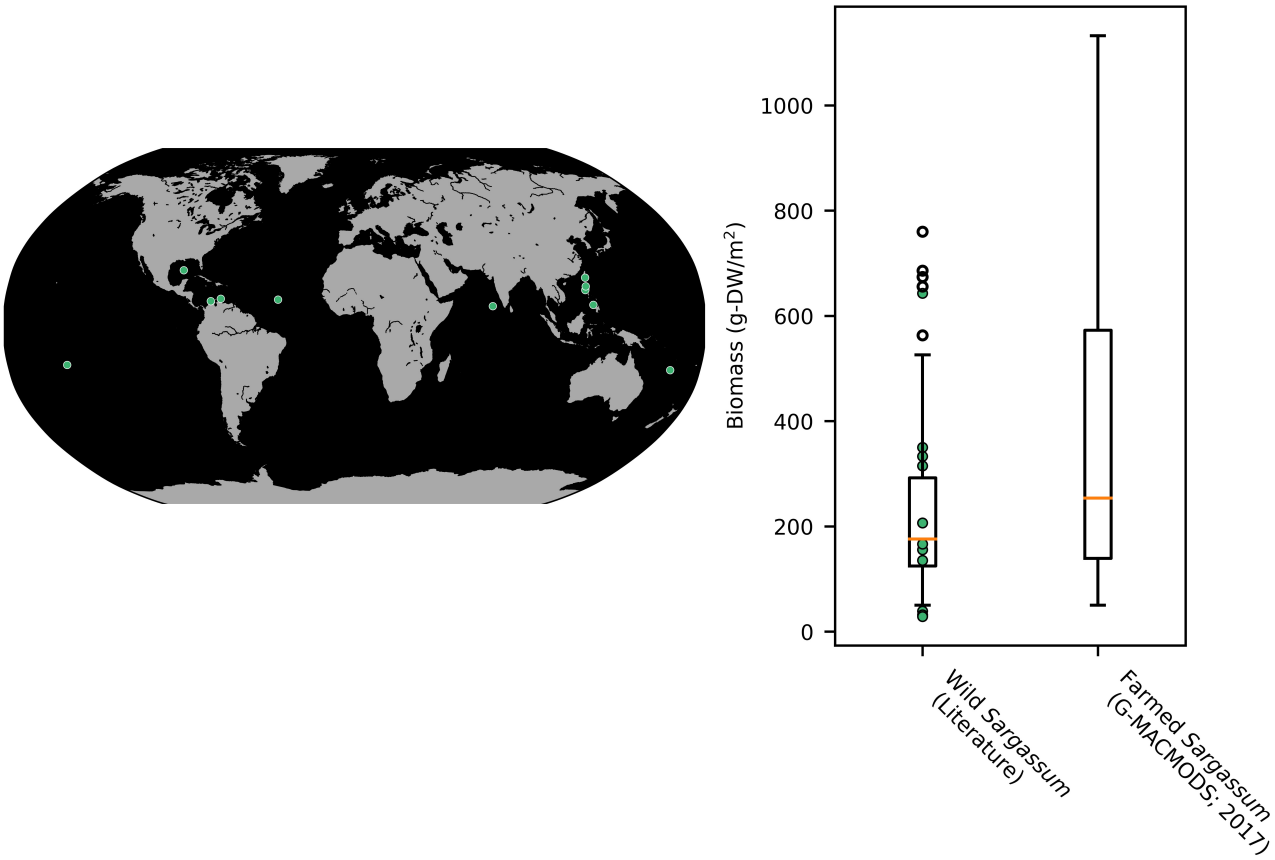


**Figure 6. Model-field comparisons (tropical brown seaweed).** Locations of wild *Sargassum* observations in 20–30 (left panel). Boxplots of wild *Sargassum* standing stock in 20–30, as well as the maximum tropical brown biomass observed in G-MACMODS ambient nutrient simulations when harvest is not imposed (to better match the wild seaweed values in the literature) are shown in the right panel. Only values above B = 50 g-DW/m$^2$ (the tropical brown seed weight in G-MACMODS) are shown in the boxplots (n = 40 values from 10 articles and > 900,000 values from G-MACMODS). Green circles indicate the mean reported biomass in the literature articles referenced above. Values reported in fresh weight were converted to dry weight by assuming a dry-to-wet biomass ratio of 1:10.

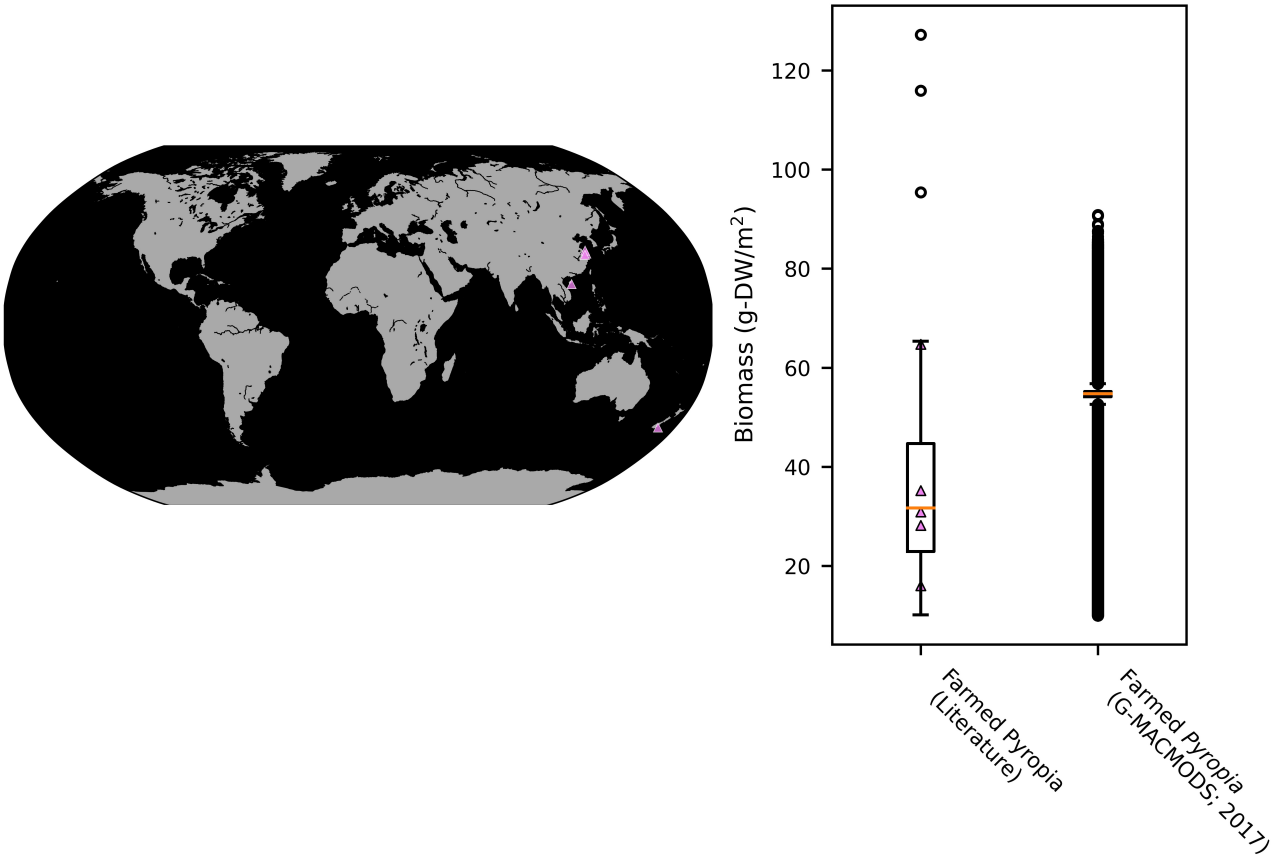


**Figure 7. Model-field comparisons (temperate red seaweed).** Locations of farmed *Pyropia* observations in 7, 12, 31–33 (left panel). Boxplots of *Pyropia* harvest in 7, 12, 31–33, as well as the maximum temperate red seaweed biomass harvested in a single harvest cycle in G-MACMODS ambient nutrient simulations (right panel). Only values above B = 10 g-DW/m$^2$ (the temperate red seed weight in G-MACMODS) are shown in the boxplots (n = 53 values from 5 articles and > 1.8 million values from G-MACMODS). Pink triangles indicate the mean harvest values in the literature articles referenced above. Values reported in fresh weight were converted to dry weight by assuming a dry-to-wet biomass ratio of 1:10.

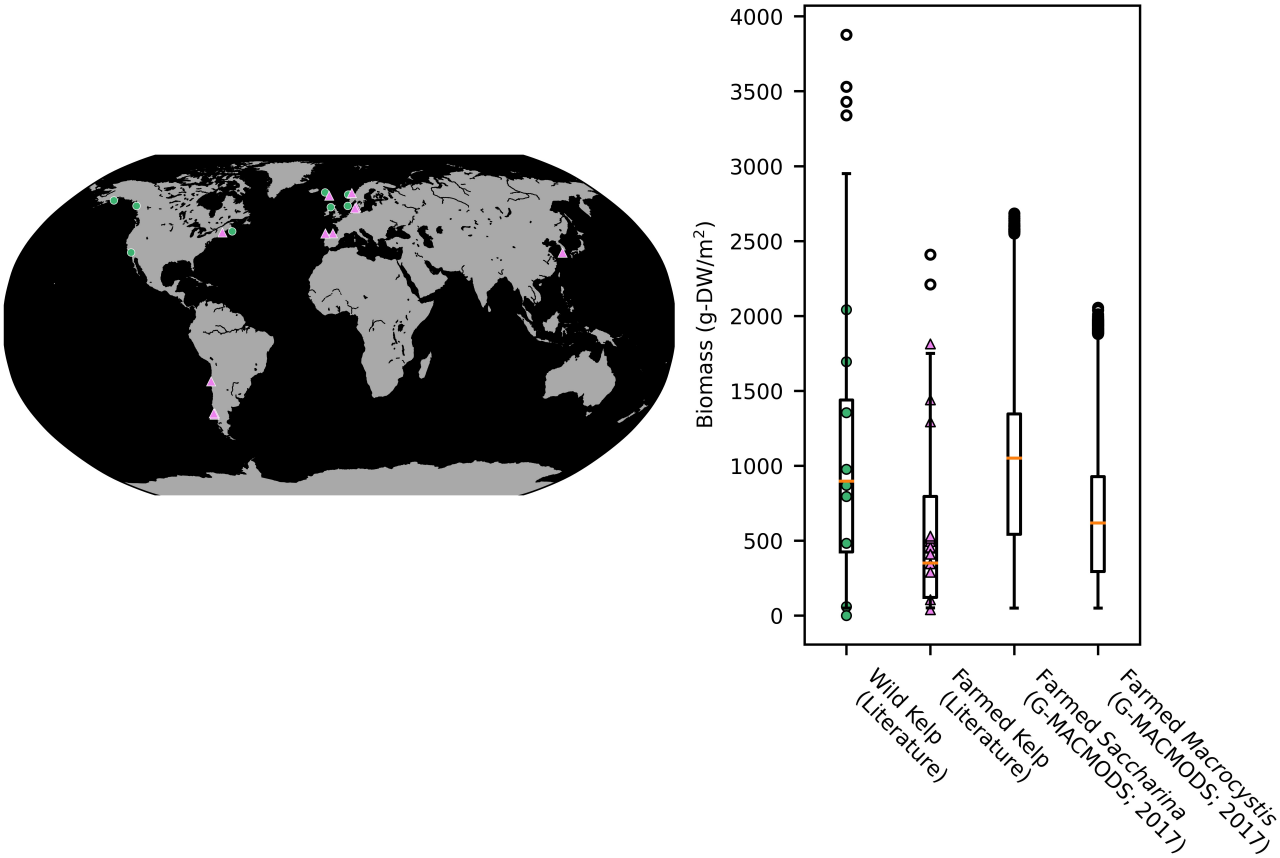


**Figure 8. Model-field comparisons (temperate brown seaweed).** Locations of wild (34–43; green circles) and farmed (44–56; pink triangles) *Saccharina*, *Laminaria*, and *Macrocystis* observations (left panel). Some neighboring locations may not be resolved (may be plotted on top of other locations). Boxplots of wild standing stock values from 34–43 (n = 127 values from 10 articles), harvest from 44–56 (n = 80 values from 13 articles), and maximum kelp biomass output from G-MACMODS (ambient nutrient scenario) when harvest is not imposed (n > 1.5 million values) are showin in the right panel. Only values above B = 50 g-DW/m$^2$ (the temperate brown seed weight in G-MACMODS) are shown in the boxplots. Green circles and pink triangles indicate the mean reported biomass in the literature articles that discuss wild and farmed kelp, respectively. Values reported in fresh weight were converted to dry weight by assuming a dry-to-wet biomass ratio of 1:10.

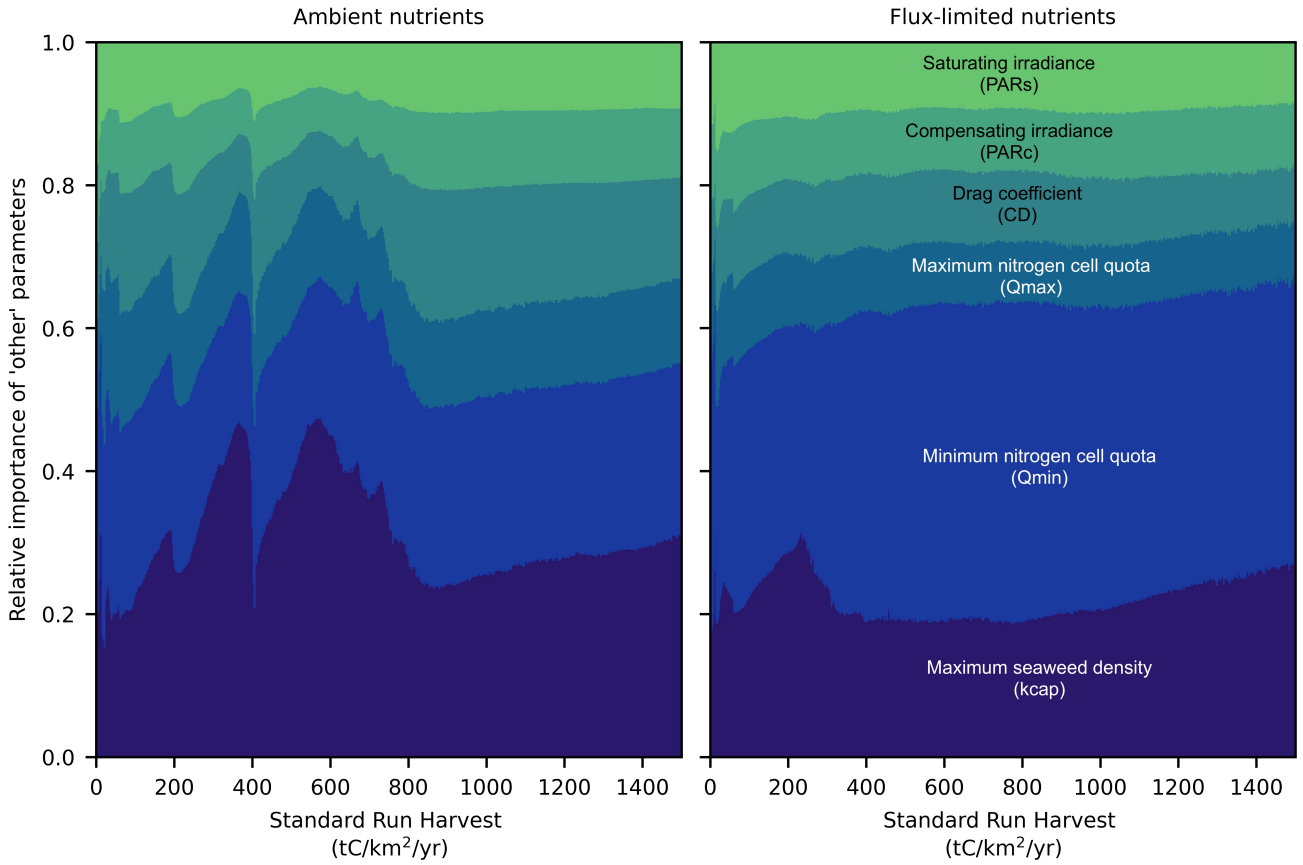


**Figure 9. Random forest results.** Focused view of the "other" category in Figure 3 of the main manuscript. The results have been normalized to reflect the relative importance of each parameter. For parameter information, please refer to Table 1 of the main manuscript.

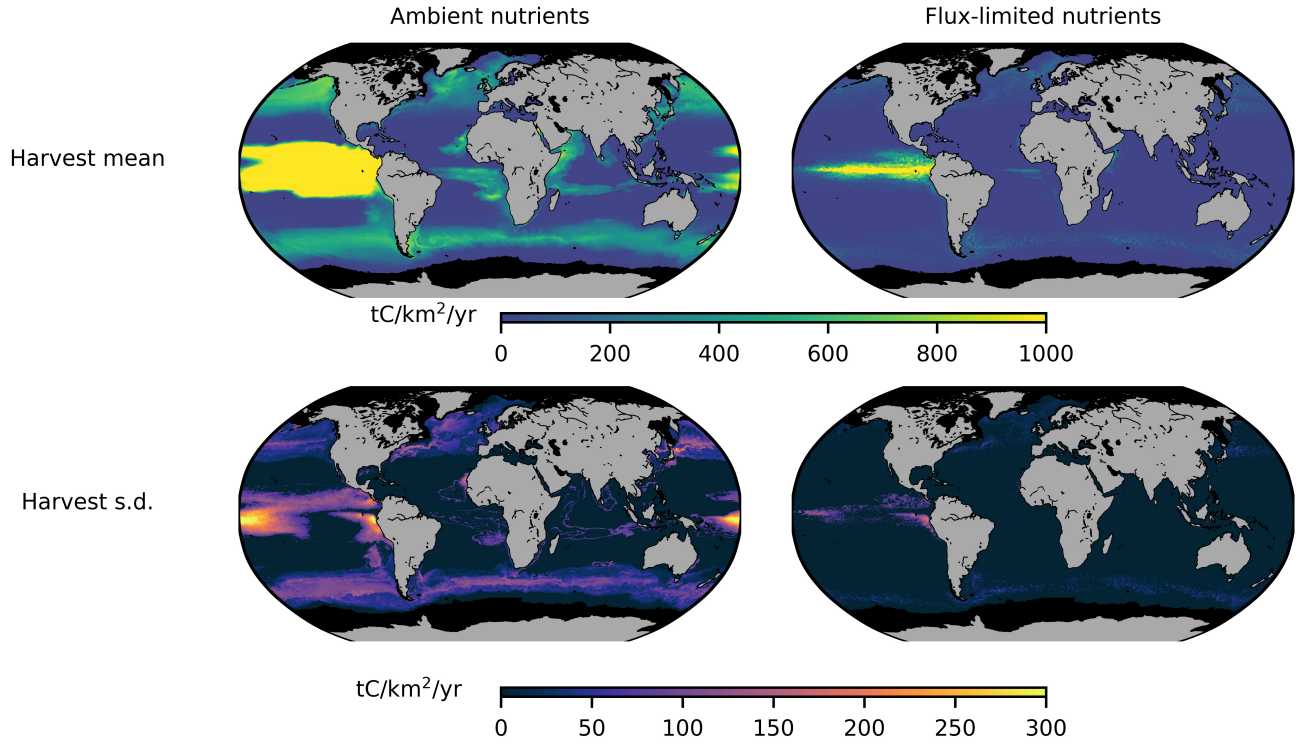


**Figure 10. Inter-annual harvest variability**. Harvest yield temporal mean (top row) and standard deviation (bottom row) across 2002–2019.

## References


1. Wakibia, J., Ochiewo, J. & Bolton, J. J. Economic analysis of eucheumoid algae farming in Kenya. *West. Indian Ocean. J. Mar. Sci.* **10**, 13–24 (2011).
2. Nugroho, R., Wijayanto, D., Kurohman, F., Maulina, I. & Puspitasari, R. The Growth Analysis of Euchema *cottonii* using The Simple Longline Method and Basket Method on The Coast of Kemojan Island. In *IOP Conference Series: Earth and Environmental Science*, vol. 750, 012056, DOI: 10.1088/1755-1315/750/1/012056 (IOP Publishing, 2021).
3. Periyasamy, C., Rao, P. S. & Anantharaman, P. Harvest optimization to assess sustainable growth and carrageenan yield of cultivated *Kappaphycus alvarezii* (Doty) Doty in Indian waters. *J. Appl. Phycol.* **31**, 587–597, DOI: 10.1007/s10811-018-1562-7 (2019).
4. Villanueva, R. D., Romero, J. B., Montaño, M. N. E. & Purita, O. Harvest optimization of four *Kappaphycus* species from the Philippines. *Biomass bioenergy* **35**, 1311–1316, DOI: 10.1016/j.biombioe.2010.12.044 (2011).
5. de Góes, H. G. & Reis, R. P. An initial comparison of tubular netting versus tie–tie methods of cultivation for *Kappaphycus alvarezii* (Rhodophyta, Solieriaceae) on the south coast of Rio de Janeiro State, Brazil. *J. Appl. Phycol.* **23**, 607–613, DOI: 10.1007/s10811-010-9647-y (2011).
6. Kumar, K. S., Ganesan, K., Rao, P. S. & Thakur, M. Seasonal studies on field cultivation of *Kappaphycus alvarezii* (Doty) Doty on the northwest coast of India. *J. applied phycology* **28**, 1193–1205, DOI: 10.1007/s10811-015-0629-y (2016).
7. Wang, X. *et al.* Economically important red algae resources along the Chinese coast: History, status, and prospects for their utilization. *Algal Res.* **46**, 101817, DOI: 10.1016/j.algal.2020.101817 (2020).
8. Juanich, G. L. Manual on seaweed farming 1. *Eucheuma* spp. (1988).
9. Ndobe, S. *et al.* *Eucheuma*toid seaweed farming under global change-Tomini Bay seaweed trial indicates *Eucheuma* denticulatum (spinosum) could contribute to climate adaptation. *Aquac. Aquarium, Conserv. & Legislation* **13**, 2452–2467 (2020).
10. Msuya, F. E. *et al.* A comparative economic analysis of two seaweed farming methods in Tanzania. *The Sustain. Coast. Communities Ecosyst. Program. Coast. Resour. Center, Univ. Rhode Island West. Indian Ocean. Mar. Sci. Assoc.* (2007).
11. Ganesan, M. *et al.* Seaweed resources in India–current status of diversity and cultivation: prospects and challenges. *Bot. Mar.* **62**, 463–482, DOI: 10.1515/bot-2018-0056 (2019).
12. Hwang, E. K., Yotsukura, N., Pang, S. J., Su, L. & Shan, T. F. Seaweed breeding programs and progress in eastern Asian countries. *Phycologia* **58**, 484–495, DOI: 10.1080/00318884.2019.1639436 (2019).
13. Hurtado, A. Q. Social and economic dimensions of carrageenan seaweed farming in the Philippines. *Soc. Econ. Dimensions Carrageenan Seaweed Farming. Fish. Aquac. Tech. Pap. No. 580* (2013).
14. Neish, I. C. Social and economic dimensions of carrageenan seaweed farming in Indonesia. *Soc. Econ. Dimensions Carrageenan Seaweed Farming. Fish. Aquac. Tech. Pap. No. 580* (2013).
15. Periyasamy, C. & Rao, P. S. Growth rate and carrageenan yield of cultivated *Kappaphycus alvarezii* (Doty) Doty in the coastal waters of Bay of Bengal at Chepala Timmapuram, Andhra Pradesh, east coast of India. *J. Appl. Phycol.* **29**, 1977–1987, DOI: 10.1007/s10811-017-1099-1 (2017).
16. Wijayanto, D., Bambang, A. N., Nugroho, R. A. & Kurohman, F. The impact of planting distance on productivity and profit of *Eucheuma cottonii* seaweed cultivation in Karimunjawa Islands, Indonesia. *Aquac. Aquarium, Conserv. & Legislation* **13**, 2170–2179 (2020).
17. Thirumaran, G. & Anantharaman, P. Daily Growth Rate of Field Farming Seaweed *Kappaphycus alvarezii* (Doty) Doty ex. P. Silva in Vellar Estuary. *World J. Fish Mar. Sci.* **1**, 144–153 (2009).
18. Rosas, E. D. V. M., Cabrera, J. A. R., León, R. E. R. & Rodríguez, J. L. N. Evaluación del crecimiento de *Eucheuma isiforme* (Rhodophyta, Gigartinales) en sistemas de cultivo suspendidos en la isla de Cubagua, Venezuela (sureste del Mar Caribe). *AquaTechnica: Revista Iberoamericana de Acuicultura.* **2**, 86–98 (2020).
19. Makwana, N. P. Growth comparison of the seaweed *Kappaphycus alvarezii* in nine different coastal areas of Gujarat coast, India. *Adv. Appl. Sci. Res.* **2**, 99–106 (2011).
20. Trono Jr, G. C. & Tolentino, G. L. Studies on the management of *Sargassum* (Fucales, Phaeophyta) bed in Bolinao, Pangasinan, Philippines. *The Korean J. Phycol.* **8**, 249–257 (1993).
21. Rani, V., Jawahar, P. & Jeya Shakila, R. Seasonal variation in biomass and distribution of brown seaweeds (Phaeophyceae) in Gulf of Mannar, Tamilnadu, India. *The Bioscan* **10**, 1123–1129 (2015).

**22.** .

**23.** Ody, A. *et al.* From In Situ to satellite observations of pelagic *Sargassum* distribution and aggregation in the Tropical North Atlantic Ocean. *PLoS One* **14**, e0222584, DOI: 10.1371/journal.pone.0222584 (2019).

**24.** Engelen, A. H., Åberg, P., Olsen, J. L., Stam, W. T. & Breeman, A. M. Effects of wave exposure and depth on biomass, density and fertility of the fucoid seaweed *Sargassum polyceratium* (Phaeophyta, Sargassaceae). *Eur. J. Phycol.* **40**, 149–158, DOI: 10.1080/09670260500109210 (2005).

**25.** Camacho, O. & Hernández-Carmona, G. Phenology and alginates of two *Sargassum* species from the Caribbean coast of Colombia. *Ciencias Mar.* **38**, 381–393 (2012).

**26.** Andrefouet, S., Zubia, M. & Payri, C. Mapping and biomass estimation of the invasive brown algae Turbinaria ornata (Turner) J. Agardh and *Sargassum mangarevense* (Grunow) Setchell on heterogeneous Tahitian coral reefs using 4-meter resolution IKONOS satellite data. *Coral Reefs* **23**, 26–38, DOI: 10.1007/s00338-003-0367-5 (2004).

**27.** Mattio, L., Payri, C. E. & Stiger-Pouvreau, V. Taxonomic revision of *Sargassum* (Fucales, Phaeophycae) from French Polynesia based on Morphological and MOlecular Analyses 1. *J. phycology* **44**, 1541–1555, DOI: 10.1111/j.1529-8817.2008.00597.x (2008).

**28.** Calumpong, H., Maypa, A. & Magbanua, M. Population and alginate yield and quality assessment of four *Sargassum* species in Negros Island, central Philippines. *Hydrobiologia* **398**, 211–215, DOI: 10.1023/A:1017015824822 (1999).

**29.** Hwang, R.-L., Tsai, C.-C. & Lee, T.-M. Assessment of temperature and nutrient limitation on seasonal dynamics among species of *Sargassum* from a coral reef in Southern Taiwan 1. *J. Phycol.* **40**, 463–473, DOI: doi.org/10.1111/j.1529-8817.2004.03086.x (2004).

**30.** Wang, M. *et al.* The great Atlantic *Sargassum* belt. *Science* **365**, 83–87, DOI: 10.1126/science.aaw7912 (2019).

**31.** He, P. *et al.* Bioremediation efficiency in the removal of dissolved inorganic nutrients by the red seaweed, *Porphyra yezoensis*, cultivated in the open sea. *Water Res.* **42**, 1281–1289, DOI: 10.1016/j.watres.2007.09.023 (2008).

**32.** Wu, H., Kim, J. K., Huo, Y., Zhang, J. & He, P. Nutrient removal ability of seaweeds on *Pyropia yezoensis* aquaculture rafts in China's radial sandbanks. *Aquatic Bot.* **137**, 72–79, DOI: 10.1016/j.aquabot.2016.11.011 (2017).

**33.** O'Connell-Milne, S. A. & Hepburn, C. D. A harvest method informed by traditional knowledge maximises yield and regeneration post harvest for karengo (Bangiaceae). *J. applied phycology* **27**, 447–454, DOI: 10.1007/s10811-014-0318-2 (2015).

**34.** Krumhansl, K. A. & Scheibling, R. E. Detrital production in Nova Scotian kelp beds: patterns and processes. *Mar. Ecol. Prog. Ser.* **421**, 67–82, DOI: 10.3354/meps08905 (2011).

**35.** Gundersen, H. *et al.* Variation in Population Structure and Standing Stocks of Kelp Along Multiple Environmental Gradients and Implications for Ecosystem Services. *Front. Mar. Sci.* **8**, 360, DOI: 10.3389/fmars.2021.578629 (2021).

**36.** van Son, T. C. *et al.* Achieving reliable estimates of the spatial distribution of kelp biomass. *Front. Mar. Sci.* **7**, 107, DOI: 10.3389/fmars.2020.00107 (2020).

**37.** Smale, D. A. *et al.* Linking environmental variables with regional-scale variability in ecological structure and standing stock of carbon within UK kelp forests. *Mar. Ecol. Prog. Ser.* **542**, 79–95, DOI: 10.3354/meps11544 (2016).

**38.** Ulaski, B. P., Konar, B. & Otis, E. O. Seaweed Reproduction and Harvest Rebound in Southcentral Alaska: Implications for Wild Stock Management. *Estuaries Coasts* **43**, 2046–2062, DOI: 10.1007/s12237-020-00740-1 (2020).

**39.** Rassweiler, A., Reed, D. C., Harrer, S. L. & Nelson, J. C. Improved estimates of net primary production, growth, and standing crop of *Macrocystis pyrifera* in Southern California, DOI: 10.1002/ecy.2440 (2018).

**40.** Muraoka, D. Seaweed resources as a source of carbon fixation. *Bull. research agency Jpn.* 59–64 (2004).

**41.** Stekoll, M., Deysher, L. & Hess, M. A remote sensing approach to estimating harvestable kelp biomass. In *Eighteenth International Seaweed Symposium*, 97–108, DOI: 10.1007/978-1-4020-5670-3_13 (Springer, 2006).

**42.** Pedersen, M. F., Nejrup, L. B., Fredriksen, S., Christie, H. & Norderhaug, K. M. Effects of wave exposure on population structure, demography, biomass and productivity of the kelp Laminaria hyperborea. *Mar. Ecol. Prog. Ser.* **451**, 45–60, DOI: 10.3354/meps09594 (2012).

**43.** Pessarrodona, A., Moore, P. J., Sayer, M. D. & Smale, D. A. Carbon assimilation and transfer through kelp forests in the NE Atlantic is diminished under a warmer ocean climate. *Glob. Chang. Biol.* **24**, 4386–4398, DOI: 10.1111/gcb.14303 (2018).

**44.** Forbord, S., Steinhovden, K. B., Solvang, T., Handå, A. & Skjermo, J. Effect of seeding methods and hatchery periods on sea cultivation of *Saccharina latissima* (Phaeophyceae): a Norwegian case study. *J. Appl. Phycol.* **32**, 2201–2212, DOI: 10.1007/s10811-019-01936-0 (2020).

**45.** Freitas, J. R., Morrondo, J. M. S. & Ugarte, J. C. *Saccharina latissima* (Laminariales, Ochrophyta) farming in an industrial IMTA system in Galicia (Spain). *J. applied phycology* **28**, 377–385, DOI: 10.1007/s10811-015-0526-4 (2016).

**46.** Augyte, S., Yarish, C., Redmond, S. & Kim, J. K. Cultivation of a morphologically distinct strain of the sugar kelp, *Saccharina latissima* forma angustissima, from coastal Maine, USA, with implications for ecosystem services. *J. Appl. Phycol.* **29**, 1967–1976, DOI: 10.1007/s10811-017-1102-x (2017).

**47.** Boderskov, T. *et al.* Effects of seeding method, timing and site selection on the production and quality of sugar kelp, *Saccharina latissima*: A Danish case study. *Algal Res.* **53**, 102160, DOI: 10.1016/j.algal.2020.102160 (2021).

**48.** Park, C. S. & Hwang, E. K. Seasonality of epiphytic development of the hydroid Obelia geniculata on cultivated *Saccharina japonica* (Laminariaceae, Phaeophyta) in Korea. *J. applied phycology* **24**, 433–439, DOI: 10.1007/s10811-011-9755-3 (2012).

**49.** Bak, U. G., Mols-Mortensen, A. & Gregersen, O. Production method and cost of commercial-scale offshore cultivation of kelp in the Faroe Islands using multiple partial harvesting. *Algal research* **33**, 36–47, DOI: 10.1016/j.algal.2018.05.001 (2018).

**50.** Peteiro, C. & Freire, Ó. Biomass yield and morphological features of the seaweed *Saccharina latissima* cultivated at two different sites in a coastal bay in the Atlantic coast of Spain. *J. applied phycology* **25**, 205–213, DOI: 10.1007/s10811-012-9854-9 (2013).

**51.** Peteiro, C., Sánchez, N., Dueñas-Liaño, C. & Martínez, B. Open-sea cultivation by transplanting young fronds of the kelp *Saccharina latissima*. *J. applied phycology* **26**, 519–528, DOI: 10.1007/s10811-013-0096-2 (2014).

**52.** Marinho, G. S., Holdt, S. L., Birkeland, M. J. & Angelidaki, I. Commercial cultivation and bioremediation potential of sugar kelp, *Saccharina latissima*, in Danish waters. *J. applied phycology* **27**, 1963–1973, DOI: 10.1007/s10811-014-0519-8 (2015).

**53.** Macchiavello, J., Araya, E. & Bulboa, C. Production of *Macrocystis pyrifera* (Laminariales; Phaeophyceae) in northern Chile on spore-based culture. *J. Appl. Phycol.* **22**, 691–697, DOI: 10.1007/s10811-010-9508-8 (2010).

**54.** Correa, T. *et al.* Production and economic assessment of giant kelp *Macrocystis pyrifera* cultivation for abalone feed in the south of C hile. *Aquac. research* **47**, 698–707, DOI: 10.1111/are.12529 (2016).

**55.** Gutierrez, A. *et al.* Farming of the giant kelp *Macrocystis pyrifera* in southern Chile for development of novel food products. In *Eighteenth International Seaweed Symposium*, 33–41, DOI: 10.1007/978-1-4020-5670-3_5 (Springer, 2006).

**56.** Camus, C., Infante, J. & Buschmann, A. H. Overview of 3 year precommercial seafarming of *Macrocystis pyrifera* along the Chilean coast. *Rev. Aquac.* **10**, 543–559, DOI: 10.1111/raq.12185 (2018).